# A STUDY ON EFFECT OF LAMINATED RUBBER – METAL SPRING ON TENSILE AND HARDNESS

MOHAMAD IKHWAN BIN MOHAMED RAZAK



UNIVERSITI TEKNIKAL MALAYSIA MELAKA

# A STUDY ON EFFECT OF LAMINATED RUBBER – METAL SPRING ON TENSILE AND HARDNESS

**MOHAMAD IKHWAN BIN MOHAMED RAZAK**

**A report submitted in fulfillment of the requirements for the degree of Bachelor of Mechanical Engineering**



**Faculty of Mechanical Engineering**

**UNIVERSITI TEKNIKAL MALAYSIA MELAKA**

**2019**

**DECLARATION**

I hereby, declared this report entitled a study on effect of laminated rubber – metal spring on tensile and hardness is the results of my own research except as cited in references.

Signature: .....

Author : Mohamad Ikhwan Bin Mohamed Razak

Date:

**APPROVAL**

This report is submitted to the Faculty of Mechanical Engineering of Universiti Teknikal Malaysia Melaka (UTeM) as a partial fulfilment of the requirements for the degree of Bachelor of Mechanical Engineering with Honours.

Signature: .....

Supervisor: Dr. Mohd Azli Bin Salim

Date:

# DEDICATION

To my beloved parents

(Mohamed Razak Bin Sheik Hamid and Sofiah Binti Hassan)

My beloved family,

(Mohamad Irfan Bin Mohamed Razak and Mohamad Irwan Bin Mohamed Razak)

My Supervisor,

(Dr. Mohd Azli Bin Salim)

My lectures,

And all my beloved friends

(Azrin Ahmadin, Muthanna Bin Jumadil, Syafiq Firdaus, Mad Haniff bin Mad Rasi, Rais Adham, Azamuddin Nasir, Fakhruddin Mutussin, Ahmad Afiq Amsyar dan Mohd Zairunshah Bin Bernados)



`

# ABSTRACT

This project is to promote SMR CV-60 as the most important substance in the development of laminated rubber metal spring (LR-MS). In order to investigate the compatibility of SMR CV - 60 as the main substance in LR-MS development, the hardness and the young modulus of SMR CV - 60 at various force (0.1, 0.2, 0.4, 0.6, 0.8, 1.0, 1.2, 1.4 and 1.6) mN are to be investigated. This thesis will describes in details the methodologies that have been used during conducting the nanoindentation testing. In order to achieve this objective, a nanoindentation test was conducted to obtained mechanical properties for NR which is SMR CV-60 in 3 different types of NR conditions which is normal test, tensile test and heat treatment before conducting nanoindentation test. The normal test refer to original condition of rubber without any testing before using nanoindentation test. Tensile test was conducted at room temperature by stretching the specimen at rate of 100, 200 and 300 mm/min before conduction nanoindentation testing. Heat treatment was carried out at temperature of 100 and 200 before conducting nanoindentation testing. The reason to conduct 3 test above was to determine the hardness and young modulus for before and after test. For normal test, the depth penetration increase as the force increase. The hardness/young modulus is unpredictable as the force increase but graph showing an increasing trend for hardness value. For tensile test 100, 200 and 300 mm/min, the depth penetration also increase as the force applied increase where the hardness/young modulus decrease after tensile test have been done to SMR CV-60. Lastly, for heat treatment, the depth penetration also increase as the force applied increase. For sample 9 where heat treatment at 100, the hardness decrease after heat treatment for both sample 9 and 10 but young modulus remain unchanged after heat treatment





`

# ABSTRAK

*Projek ini adalah untuk mengkaji kebolehan SMR CV-60 sebagai bahan yang paling penting dalam pembuatan Laminated Rubber-Metal Spring (LR-MS). Untuk mengkaji keberkesanan SMR CV - 60 sebagai bahan utama dalam pembangunan LR-MS, kekerasan dan young modulus SMR CV-60 pada pelbagai daya (0.1, 0.2, 0.4, 0.6, 0.8, 1.0, 1.2, 1.4 dan 1.6) mN akan dijalankan. Tesis ini akan menerangkan secara terperinci metodologi yang telah digunakan semasa menjalankan ujian nanoindentation. Untuk mencapai matlamat ini, ujian nanoindentation dilakukan untuk mendapatkan sifat mekanikal untuk Natural Rubber (NR) yang merupakan SMR CV-60 dalam 3 jenis keadaan Natural Rubber NR yang berbeza iaitu keadaan normal, ujian tensile dan rawatan haba sebelum menjalankan ujian nanoindentation. Ujian normal merujuk kepada keadaan asal getah tanpa sebarang ujian sebelum menggunakan ujian nanoindentation. Ujian tensile dilakukan pada suhu bilik dengan menarik spesimen pada kadar 100, 200 dan 300 mm / min sebelum pengujian nanoindentation dijalankan. Rawatan haba dilakukan pada suhu 100 ℃ dan 150 ℃ sebelum melakukan ujian nanoindentation. Sebab untuk menjalankan 3 ujian di atas adalah untuk menentukan kekerasan dan young modulus sebelum dan selepas ujian. Bagi ujian biasa, penembusan kedalaman meningkat apabila daya meningkat. Kekerasan / young modulus tidak dapat diprediksi memandangkan peningkatan daya tetapi graf menunjukkan peningkatan trend untuk nilai kekerasan. Untuk ujian tegangan 100, 200 dan 300 mm / min, penembusan kedalaman juga meningkat apabila daya digunakan meningkat di mana kekerasan / young modulus menurun selepas ujian tegangan telah dilakukan ke SMR CV-60. Akhir sekali, untuk rawatan haba, penembusan kedalaman juga meningkat apabila daya digunakan meningkat. Untuk sampel 9 di mana rawatan haba pada 100℃, kekerasan menurun selepas rawatan haba untuk kedua-dua sampel 9 dan 10 tetapi young modulus kekal tidak berubah selepas rawatan haba.*



`

# ACKNOWLEDGEMENTS

To my beloved lecturer and supervisor, who always provide me guidance, advices and idea along the way to develop this experiment. The unconditionally sharing of knowledge allows me to learn plenty of new things. Many thanks to Dr. Mohd Azli Bin Salim as my supervisor for the assistance and patience. Lastly, I would like to thank everyone who assists me from the beginning till the end of this Final Year Project.

Thank you.





`

# TABLE OF CONTENTS

`

`

# LIST OF TABLES







`

# LIST OF FIGURES

`

# LIST OF ABBREVIATIONS

| | | |
|---|---|---|
| $mN$ | - | Micro newton |
| $\mu N$ | - | Micro newton |
| $\mu m$ | - | Micro meter |
| $h_{max}$ | - | Maximum depth |
| $P_{max}$ | - | Maximum force |
| $h_p$ | - | Penetration depth |
| $h_c$ | - | Depth of contact |
| $h_e$ | - | Displacement associated with the elastic recovery during unloading |
| $E_r$ | - | Converted elastic modulus |
| $E_i$ | - | Initial elastic modulus |
| $V_i$ | - | Poisson's ration for indenter |
| $E_{it}$ | - | Indentation elastic modulus |
| $V_s$ | - | Poisson's ratio for specimen |
| $r$ | - | Radius |
| $A_r$ | - | Area |
| $A_l$ | - | Aluminium |





`

# CHAPTER 1

# INTRODUCTION

## 1.0 Introduction

This section will explain more about the context of this experiment, a study on the impact of laminated rubber – metal spring on tensile and hardness consisting of natural rubber history in Malaysia and the use of natural rubber in engineering applications that focus on vibration isolator This section will illustrate the mechanical characteristics, material utilization and implementation of the two common natural rubbers, Standard Malaysian Rubber (SMR) and Epoxidized Natural Ruber (ENR).

## 1.1 Background Study

Nowadays, natural rubber (NR) is a versatile and adaptable material because in 150 years, it was successfully used in many engineering applications. It is a type of sustainable material and very popular in Malaysia as well as around the world for many applications1 such as in the automotive industry, manufacturing, civil, railways, offshore, aerospace, and defense. It becomes an important material due to its ability to withstand large deformations and store more elastic energy per unit volume compared with other elastic materials (Salim, Putra, Mansor, Musthafah, Akop, Abdullah, et al., 2016). It also has characteristic damping in term of vibration resonance. NR also has a unique response which is small compressibility during the application of excitation force. By adding other





`

materials inside the NR, it will be known as the composite material (Salim et al., 2016). A rubber bearing was introduced to become isolator to suppress the amount of vibration particularly in building structure for earthquake protection. It is made up from layers of rubber with thin steel plates between them, and a thick plate located at above and bottom of the rubber materials. These rubber bearings are set between the bottom of a building and its foundation by embedding the metal plates that will provides excellent performance in terms of stress and strain level once high load is applied and prevents the bulging impact within the horizontal direction. It's designed to be really stiff and powerful for vertical load, so it able to accommodate the extreme weight of the building strain level once the high load is applied and prevents the bulging impact within the horizontal direction.

Epoxidized Natural Rubber (ENR), the epoxidation method was a major option as it exhibits a simple reaction procedure and effective compounding cost. The epoxidation process involving the addition of oxygen atom into a proportion of carbon-carbon double bonds through the addition or substitution reaction to produce the epoxide ring. This process is more effective when conducted at the latex stage by using several chemicals such as the performic acid, the hydrogen peroxide, and the formic acid. The performic acid is a soluble liquid with strong oxidizing properties. The NR can be epoxidized up to 75 mole % under a controlled condition to produce NR compound with superior properties such as better resistance towards the hydrocarbon oil and high mechanical properties. However, the epoxidation of NR up to 100 mole% will produce hard thermoplastic materials (Baker et al., 2014). The advantages of ENR over the other modified NR are the outstanding damping properties, high resistance to hydrocarbon oils,



`

good strength properties, high wet grip and lower air permeability. For this reasons, the ENR has been used in various application such as automotive tire tread, adhesive, bladders, vibration mount, and shoe soles. Besides that, the epoxidation process has supplied the ENR with high glass transition temperature and high polarity. High polarity in ENR makes it suitable to be used with the vulcanized NR with different polarity and bonded with metals (Baker et al., 2014). Currently, only two types of ENR was commercially used which is the ENR 25 and ENR 50. In Malaysia, the ENR was commercialized by Malaysian Rubber Board (MRB) under the name of Ekoprena 25 and Ekoprena 50. The physical properties for ENR 25 and the ENR 50 was summarized and presented in Table 1.1.

Table 1.1: The physical properties for ENR 25 and the ENR 50

| **Property** | **SMR CV-60** | **ENR 50** |
|---|---|---|
| Tensile strength (MPa) | 22.4 | 21.0 |
| Elongation at break (%) | 497 | 465 |
| Rebound Resilence, at 23°C (90) | 39.7 | 25.9 |
| Compression set (72hr, RT) (%) | 16.5 | 20.5 |
| Tear strength (N/mm) | 94.0 | 57.0 |





`

Standard Malaysian Rubber Constant Viscosity (SMR CV), variety grade of coagulated NR compound was available and all of them have been technically specified according to the American Society for Testing Materials (ASTM). All coagulated compound were measured based on its physical properties such as the dirt content and the method of production. However, the detailed description of the NR also can be obtained through the respective rubber producing country. As in Malaysia, the basic grades of coagulated NR compound were promoted as Standard Malaysian Rubber (SMR) The SMR 5, SMR 10, SMR 20, SMR GP and SMR L are the examples of NR compound under the SMR scheme. In order to obtain the consistency in viscosity of the NR latex, a specialized grade with a constant viscosity (SMR CV) was introduced. The constant viscosity properties were also available for the SMR grade and the product was labeled as SMR 10CV and SMR 20CV The SMR CV grade contains about 0.15% of hydroxylamine hydrochloride or hydroxylamine neutral sulfate. The main purpose of the chemicals addition is to maintain the viscosity of the raw rubber liquids in order to prevent rubber hardening during the storage period. Rubber hardening could occur due to the reaction of the particle crosslinking process with the low humidity in storage surrounding. The SMR CV-50 and SMR CV-60 are the examples of SMR CV grade that is commercially available. The only differences between both types of constant viscosity NR are their Mooney viscosity values 50 and 60 Mooney unit. The tensile properties of the rubber blend were presented in Table 1.2





`

Table 1.2: The tensile properties of the rubber blend

| **Property** | **Blend ratio, MPa (SMR CV-60 to ENR 50)** | | | | |
|---|---|---|---|---|---|
| | **0/100** | **25/75** | **50/50** | **75/25** | **100/0** |
| Tensile strength (MPa) | 10.70 | 9.50 | 12.50 | 14.00 | 13.20 |
| Elongation at break (%) | 700 | 700 | 700 | 700 | 700 |
| Tensile modulus at 300% of elongation (MPa) | 1.65 | 1.60 | 1.60 | 1.70 | 2.60 |

## 1.2 Problem Statement

Before this, it was found that the development of the laminated rubber-metal spring (LR-MS) for the application of automotive mounting is in current trend (Salim et al., 2015). The objective of LR-MS is to reduce the vibrations in some specific portion of the receiver structure. Previously, many engineers failed to choose the appropriate rubber to be used as laminated for the rubber bearing. The rubber used has weak in mechanical properties such as hardness and young modulus. Therefore, this study is conducted to study the application of the Malaysian NR which is the vulcanized standard Malaysian rubber constant viscosity 60 (SMR CV-60) reinforced with carbon black (CB) as the potential main materials to be combined with the metal plate for the development of LR-MS has become the interest. This study focuses on the investigations of the mechanical properties of the vulcanized SMR CV-60 through the nanoindentation testing. The properties of the SMR CV-60 were compared for three types of testing that have been done to the SMR CV-60 which is normal test, tensile test and heat treatment.





`

## 1.3 Objective

The objectives of this project are:

i. To investigate and evaluate the tensile properties of SMR CV – 60

ii. To determine the relationship between tensile properties and hardness of SMR CV - 60

## 1.4 Scope of Project

Based on the objectives of the study, several scopes covered in this project are listed as below:

i. The experiment only use SMR CV-60 as the main material for mechanical testing.

ii. This study only obtain the mechanical properties (hardness and young modulus) for natural rubber using nanoindentation method

iii. The force applied to the natural rubber (NR) is varied for force (0.1, 0.2, 0.4, 0.6, 0.8, 1.0, 1.2, 1.4 and 1.6) $\mu N$



iv. The orientation of SMR CV-60 only in Y-axis for tensile test

## 1.5 Report Organization

This report is cover by five chapters. The first chapter start with the introduction, problem statement, objective and scope of project. The literature review is discussed in Chapter 2 and project methodology in Chapter 3. The result and collection of data will be discussed in Chapter 4. In Chapter 5 will be the summary of this project with some recommendation. Here are the main chapters for this project



`

In chapter 1 will covered the background of the overall operation, the problem statement that happened before this. The aim of the objective of this project is to solve the problem statement. Besides, the scope of work is limitation of project to prevent future problem.

In chapter 2 will covered the research, find and read relevant topics from the sources such as reference book, internet and journal to get deeper knowledge and information for the project. Research on the same system that already in the market to know the characteristics of the system will provide understanding in this project.

In chapter 3 will explains more about the work flow of the development of this project from the beginning of the project until the end of the project. The flow chart is used as to visualize the work flow of this project. The purpose is to have a guideline while conducting this project.

In chapter 4 will focuses on the result and the findings of the study, the results is obtained after following the methodology in the Chapter 3. It will discuss briefly on the project findings in this chapter.

In last chapter which is chapter 5 will summarize for the outcomes of this experiment. Besides, it will discuss several recommendations for future improvements and development.





`

# CHAPTER 2

# LITERATURE REVIEW

## 2.0 Introduction

As mentioned in the previous chapter, the development of the Laminated Rubber-Metal Spring (LR-MS) for the application in high-frequency protection was in the current research interest. Therefore, the Malaysian Rubber Board (MRB) has taken an initiative to optimize the usage of local grade Natural Rubber (NR) instead of imported rubbers in the development of the Laminated Rubber-Metal Spring (LR-MS), by introducing the SMR CV-60 as the main substance. Thus, in this chapter, the theories and the advantages of the Standard Malaysian Rubber (SMR CV-60). The theories of mechanical testing of the Natural Rubber (NR) were also literally presented in this chapter. In addition, a brief introduction to the nanoindentation theories and studies were included in this chapter. Lastly, the basic concept of the vibration isolation system and the history and recent studies on the laminated rubber bearing were also included to prove the effectiveness of NR as main substance in the LR-MS



## 2.1 Natural Rubber as the Sustainable Green Materials

The NR has been extensively used in various applications due to its distinctiveness over the other materials like excellent physical properties, renewable sources origins, and economical. The elasticity and the flexibility of the NR are the main reasons for this



`

material to be applied in various fields especially in the engineering area. In addition, the ability of NR to withstand for exceptional large stress without permanent deformation or fracture has ensured the survival of the materials itself and makes it suitable to be used in variety environment, except for the environment that exposed to the ozone and chemicals.

Table 2.1: Application and properties of NR

| Application | Properties |
|---|---|
| Surgical gloves | Tear resistance, strain induce crystallization |
| Blow-out preventers, hoses connectors, inner tubes, and bladders | Oil-resistance, gas permeability |
| Tires | Tear strength, wet-grip, rolling resistance/abrasion |
| Bearings | Elasticity, low dissipation factor, wear resistance |
| Shoes | Damping |



The basic strength of the NR actually depends on its basic chemical structure. Like the other natural product such as cellulose and silk, the NR was categorized as high polymer materials. The NR, which was classified in the hydrocarbon group is 99% build up from the poly-isoprene arranged in a high cis-1, 4 configurations as shown in Figure 2.1 in below. The presence of such a chemical configuration gives the NR a glass transition temperature of approximately -75 C, which makes NR become extremely elastic and works very well at room temperature (Chandrasekaran, 2010). It also



`

manifests the NR with the ability to undergo for strain-induced crystallization that leads to excellent tensile strength and great resistance towards tearing and abrasion. In addition, the NR also has high bulk modulus due to relative strong intermolecular forces in the NR compound with the value around 10000 MPa and the Poisson's ratio value of 0.499 (Tabor, 1994). Due to the high bulk modulus value, the NR was assumed as nearly incompressible when b compressed in the solid state.

(Carter & Giles F. Carter and Donald E. Paul, 1991) describe the mechanical properties of the NR in the terms of stress and strain curve as shown in Figure 2.1. Based on the figure, the curve exhibit for two different phases; first, the large elongation at the low-stress phase and second, the small elongation at large phase. During the first phase, low stress was needed to stretch the coiled polymer network and causing the curve to exhibits for small Young's Modulus reading. Besides that, in this state, the NR was able to return to its original shape or length. Meanwhile in the second phase, as the strain was continuously applied, the NR networks were started to uncoil and stretched to its maximum. Thus, higher stress was needed to stretch the NR, which is resulting in higher Young's Modulus reading. In response to the applied stress, some of the NR networks have become fully extended and unable to withstand the applied stress. This would lead to the permanent changes or deformation in the NR. The behaviors of the network polymer were illustrated in Figure 2.1, as below





`

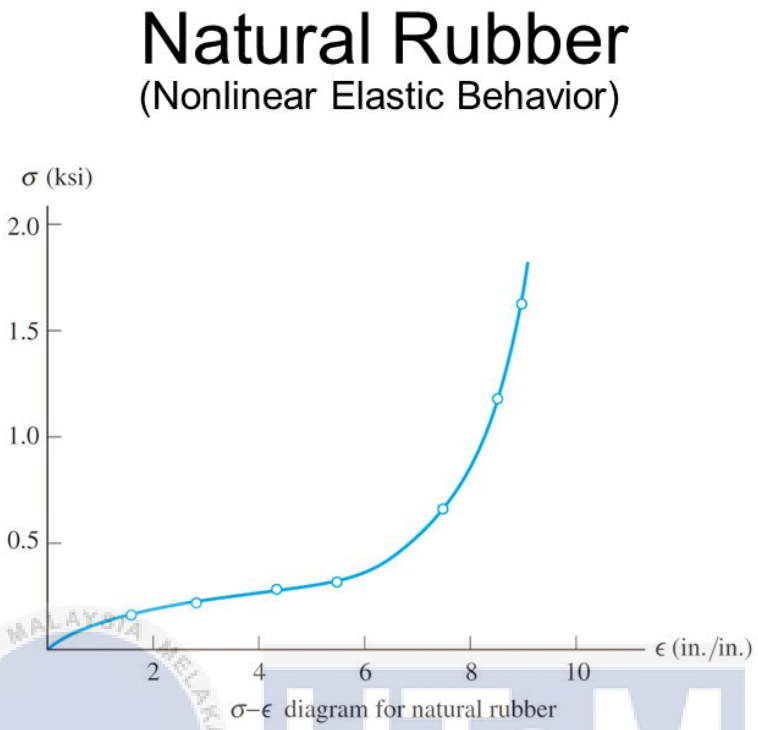


Figure 2.1 The nonlinear stress versus strain curve for the NR (Carter & Giles F. Carter and Donald E. Paul, 1991).

Based on the figure, the retraction curve was produced under the extension curve, which indicates for the rubbers behaviour during the unloading process. The differences between the extension and the retraction stress values under similar strain value (Δσ) represent for the hysteresis in rubber. The hysteresis behaviour happened due to internal friction between the rubber particles, which reacted towards extension and retraction. During the extension of rubber, work was increased as the area under the curve was increased and high energy was required to perform work. Meanwhile, during the retraction, less energy was needed to perform work. Thus, the excessive energy that equivalent to the area in the



`

curve loop was converted into heat. The larger the loop, the higher the energy was released; thus, indicated less elastic of NR. The hysteresis can be observed in both natural and synthetic rubbers. In the case of the NR, hysteresis was highly affected by the types of reinforcing filler, the fillers amount, and the test strain rate. Pure NR exhibits less hysteresis than the filled NR since it was more elastic.

## 2.2 Application of the NR in vibration isolation

The main objective of vibration isolator is reducing excessive vibration transmission from the source of excitation to the body. Vibration isolator has been installed in most mega-structures, such as tall buildings, bridges and offshore jacket platforms. Figure 2.6 represent a simple vibration isolation concept in form of lumped element system.

Consider a machine with mass m mounted on a structure by an elastic support with steadiness k and constant damping c. As shown in Figure 2.2, a single degree of freedom model can be assumed. The transmissibility $T_f$ is defined as the ratio of the force transmitted to the structure to the excitation force excited by the machine transmitted force, $f_t(t)$ injected to the structure to the excitation force, $f_e(t)$ excited by the machine.





`

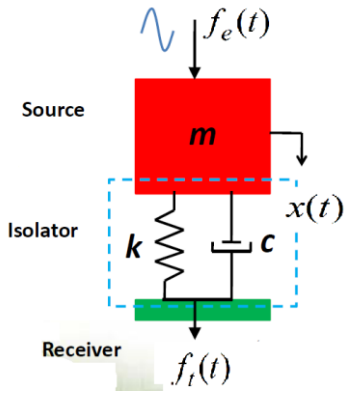


Figure 2.2: The structure to the excitation force excited by the machine

The equation of motion can be obtained by using Newton's second law given as

$$\frac{d^2x(t)}{dt^2} + c\frac{dx(t)}{dt} + kx(t) = f_e(t) \tag{1}$$

Assuming the force is harmonic, then $f_e(t) = F_e e^{j\omega t}$ and $x(t) = Xe^{j\omega t}$ where $F_e$ and $X$ are the complex amplitudes and $\omega$ is the excitation frequency.

$$F_e = (-\omega^2 m + j\omega c + k)X \tag{2}$$



Substituting this to Eq.(1) gives similarly for the transmitted force, one can obtain

$$F_t = (k + j\omega c)X \tag{3}$$

Dividing Eq. (3) with Eq.(2), the transmissibility of the model is obtained which is written as

$$T_f = \left|\frac{F_t}{F_e}\right| = \left|\frac{k + j\omega c}{k - \omega^2 m + j\omega c}\right| \tag{4}$$

Substituting $\omega_n^2 = k/m$ and $c = 2\xi\omega_n m$ into Eq. (4) to show the relation between transmissibility and damping ratio, natural frequency and operating frequency

$$T_f = \left| \frac{1 + j2\xi \dfrac{\omega}{\omega_n}}{1 - \left(\dfrac{\omega}{\omega_n}\right)^2 + j2\xi \dfrac{\omega}{\omega_n}} \right| \tag{5}$$

when model is being excited at its resonance, i.e at $\omega = \omega_n$, the transmissibility is given by

$$T_f = \frac{1}{2\xi} > 1 \tag{6}$$

Eq. (5) shows that the force received by the receiver is amplified when it is being excite near or at its natural frequency as shown in Figure 2.3. This will cause vibration to the surrounding and noise if there is no proper isolation. If this condition prolong, it will cause damage to the machine and cause structure failure.

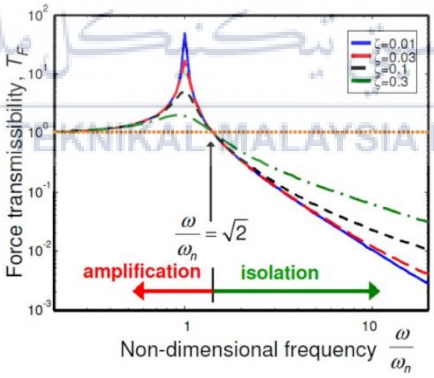


Figure 2.3: Transmissibility against non-dimensional frequency.





`

### 2.2.1 Classes of the vibration isolator

The isolation system can be divided into two classification system. First, the frictional-type sliding insulator and second, the laminated rubber bearing isolator (Ibrahim, 2008). The cutting model for both insulating classes shown in figure 2.4 below:

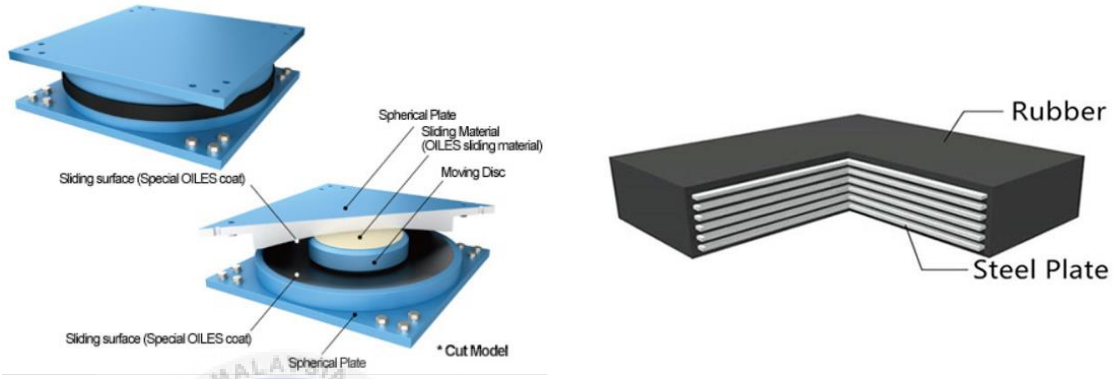


(a) (b)

Figure 2.4: Cut model of isolators (a) frictional –type sliding isolator, (b) laminated bearing isolator (Oiles Corporation, 2017)



### 2.2.2 Laminated Rubber Bearing

Laminated Rubber Bearings (LRB) consist of a laminated rubber and steel bearing for mounting to the structure with steel flange plates. The isolator's rubber acts as a spring. The LRB was built through the vulcanization process of alternate layers of rubber block and metal plates provide sufficient stiffness in the vertical direction to support the building load and flexibility in the horizontal direction to hold the ground motion during an earthquake. The metal plates providing sufficient stiffness in the vertical direction to



`

support the building load and flexibility in the horizontal direction during an earthquake. The LRB was built through the vulcanization process of alternating layers of rubber block. At the beginning of development, the LRB was designed to give the mounted structure a vertical natural frequency of 7Hz and horizontal natural frequency down to 0.4 Hz (Lindley, Fuller, Muhr, & Association., 1992)

### 2.2.3 Laminated Rubber – Metal Spring

Laminated Rubber-Metal Spring (LR-MS) has an ability to block vibration energy from rotational and longitudinal direction. Based on (Salim et al., 2015), an early study was carried out on the development of laminated rubber-metal spring (LR-MS). The objective of this study is to investigate the transmissibility of the spring in the axial direction using a multi-degree modelling of the lumped parameter system. The studies showed that the spring's isolation performance was improved by increasing the number for the degree of freedom. A vertical vibration input was applied to the LR-MS model and the stress-strain distribution and the isolator safety factor were observed. Throughout the stress-strain history, it was found that the maximum deformation values of the isolator can be reduced by embedding more metal plate's layer. In despite, the increasing of metal layers in the spring was found to generate higher stress distribution in the spring compared to the model with solid number.





`

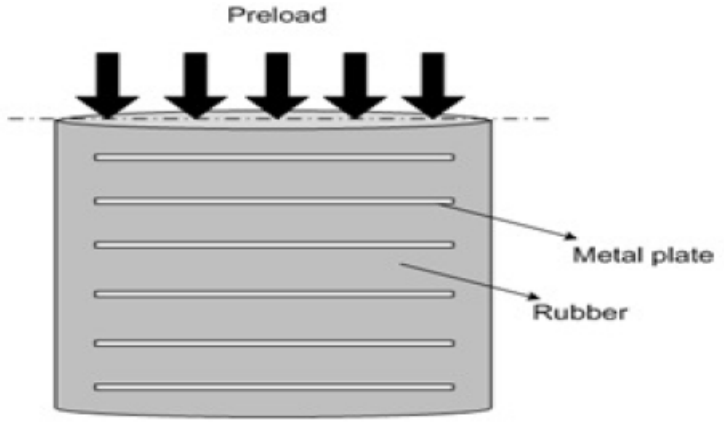


Figure 2.5: Laminated rubber - metal spring (Salim et al., 2015)

### 2.2.4 One degree of freedom (LR-MS)

A single mass connected to a spring can described a simple vibration system. The mass can only travel along the spring direction. This systems are called *Single Degree-of-Freedom* (SDOF) systems



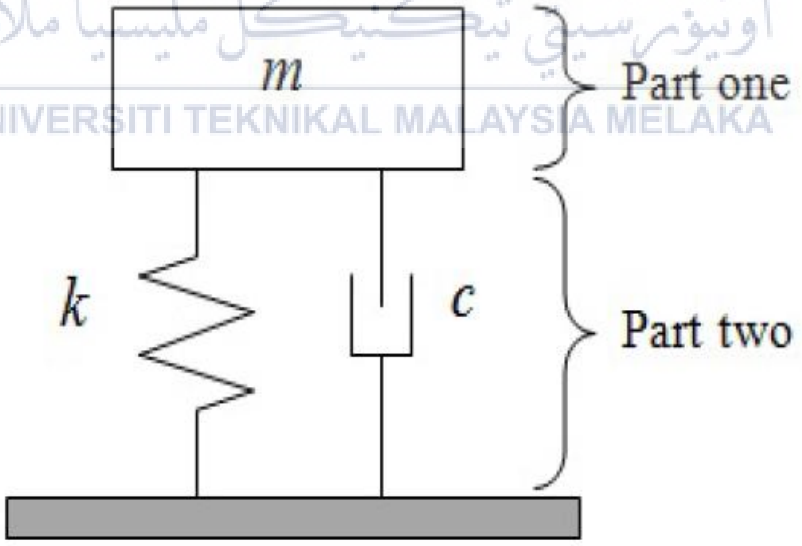


Figure 2.6: Single degree of freedom (LR-MS) (Salim et al., 2015)



`

Part one represent metal and part 2 represent natural rubber. The parameter that are really important for metal is only mass while parameter that are important for natural rubber are stiffness and damping coefficient

### 2.2.5 Two degree of freedom (LR-MS)

Two degree of freedom systems can be defined as a system that require two indent coordinates to explain their motion.

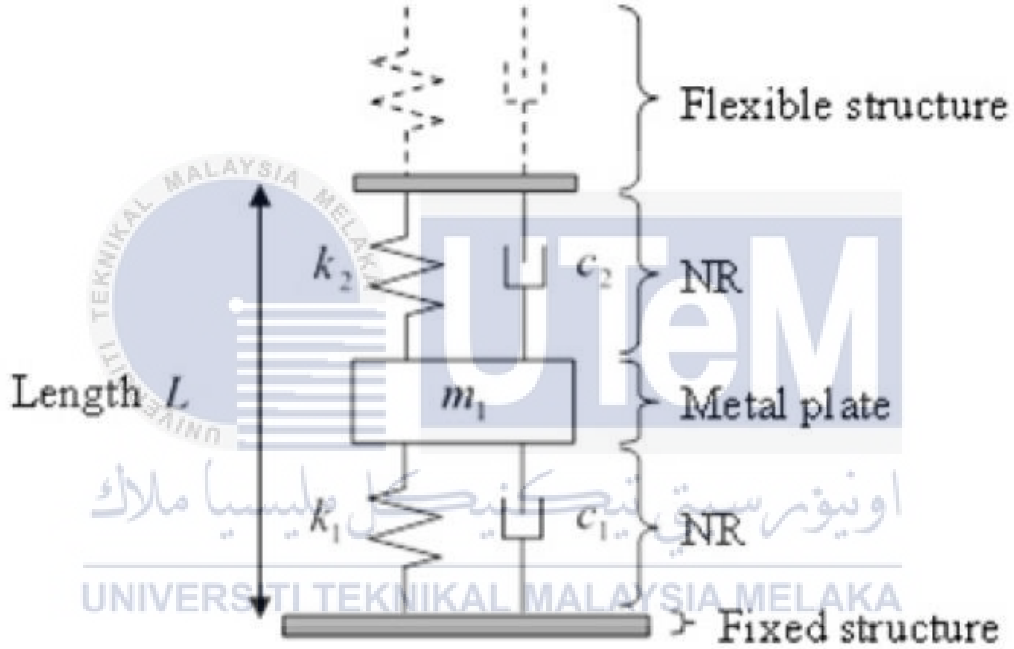


Figure 2.7: Two degree of freedom (LR-MS)

The flexible structure is designed to easily vibrate the surface and represent the free LR-MS boundary condition. The fixed structure representing the fixed limits and no displacement occurs



`

### 2.2.6 Parameter selection

$$\omega_n = \sqrt{\frac{k}{m}} \tag{7}$$

The most important parameter is the mass. The natural frequency is the rate at which an object vibrates when the external force does not disturb it. In fact, every degree of an object's freedom has its own natural frequency. Stiffness and mass are the two parameter that influenced the natural frequency. Mass is inversely proportional to the natural frequency. So, as mass increase, the natural frequency will decreases. Besides, the stiffness is directly proportional to the natural frequency. As the stiffness become high, natural frequency will also high. Second most important parameter is young modulus. Young modulus for laminated – rubber metal spring can be define as

$$k = \frac{EA}{L} \tag{8}$$



This equation shows that the value of stiffness is directly proportional to the modulus of the young modulus, provided that the quantity of the area and length of the material is in the same set of values. Stiffness is very important in principle for determining the resistance offered by an elastic body to deformation because as the stiffness value increases, the elasticity of the material will also increase. Radius is also one of the important parameters in this study because the quantity of the area of a material



`

can be determined using the radius value. Based on this experiment, LR-MS is presented in a rod-shaped where the area can be determined by using the equation below.

$$A = \pi r^2 \tag{9}$$

Based on the equation above, the area's value is directly proportional to the radius. That's mean, if the radius is increased the area also will increase, and if the value of radius decreases, the quantum of area is will decreased. This relationship can only be applicable only to the material in the form of rods only because the above equation is applicable to rods only.

## 2.3 Nano indentation theory

Nanoindentation is a variety of hardness indentation tests for small volumes. Indentation was the most commonly used for testing the mechanical properties of materials such as rubber, metal and alumminium (Broitman, 2017). In the mid-1970s, the nanoindentation technique was conducted to measure the hardness of small volumes of material (Poon, Rittel, & Ravichandran, 2008). For traditional indentation test which are macro or micro indentation, a hard tip whose mechanical properties are known (frequently made of a very hard material like diamond) is pressed into a sample whose properties are unknown. The force increase as the tip going down into the specimen. At this point, the load may be held constant for a period or removed. The residual indentation area in the sample was measured and the hardness, H, is defined as the maximum load, $P_{max}$, divided by the residual indentation area, $A_R$ :





`

$$H = \frac{P_{max}}{A_R} \tag{10}$$

The schematic diagram for the cross – section of the indenter tip in contact with testing materials was presented in figure 2.8. Based on the figure 2.8, the maximum displacement of the indenter tip into the material at the maximum applied load and the permanent recovered displacement after the tip removed was represent as $h_{max}$ and $h_p$. While, the interception of the tangent line drawn at the beginning of the unloading curve, as well as the depth where the tip and the material are in contact under the applied force, was presented as $h_c$. Besides that, $a$ was referred to the specific angle of the indenter tips that varied depending on the tip geometry. The radius of the indenter was presented as $a$.



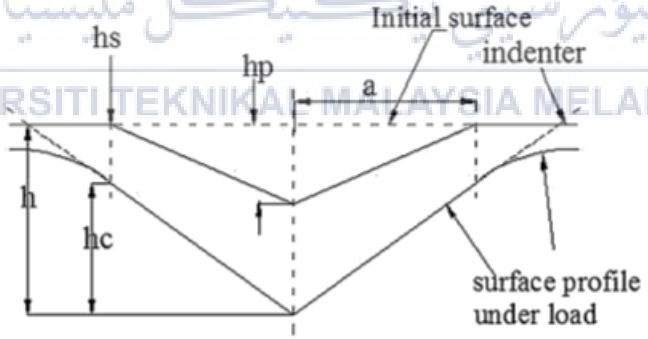


Figure 2.8: Cross – section of the indenter tip (Wu et al., 2015).



`

### 2.3.1 Load displacement curve

Nanoindentation load-displacement curves (often referred to as P-h or P-c curves) are the material response reflected in the continuous measurement of penetration depth while the load increases from zero to maximum load (loading curve) and then decreases from maximum load to zero (unloading curve). According to (Page & Hainsworth, 1993), A " micromechanical " of the material is provided by the mechanical response of the sample material impressed by a hard indenter during the indentation cycle. The obtained fingerprint has two portions; the loading portion of the curve which provides information on the materials response to strain, such as elastic, plastic and in some case phase transformation deformation and the unloading portion of the curve, which represents the elastic recovery of the material while the applied load is being removed. A material's response to the applied load in this initial stage, of loading is elastic and in this stage if the applied load is removed the deformation will be reversible and non-permanent. Eventually, when the applied load is large enough and passes the initial stage, a finite numbers of atomic bonds are broken by the movement of dislocations and some atoms will form bonds with new neighbours. If the bond breaks for a large number of atoms and they move in relation to each other, they cannot return to their original position even if the stress is removed, so the strain is permanent and called the plastic deformation (Wong & Louis, 2001). Depending on the stress response of a material during the nanoindentation test, the transition between elastic and plastic deformation may be different and may occur at different loads for different materials. When the indentation reaches the maximum applied load and plastic deformation has already taken place then during the load removal, the elastic recovery of the sample forms the unloading portion





`

of the curve. The elastic recovery of materials can be divided in to three categories; materials with a low elastic recovery, medium elastic recovery and finally materials with very high elastic recovery. Materials with low elastic recovery such as aluminium ($Al$) produce an approximately a linear unloading curve and mechanical properties of such materials can be easily provided by measurement of the unloading curve. The second type of materials, such as copper ($Cu$), provide a non-linear unloading plot due to the greater elastic recovery compared to the first type. The mechanical properties of these types of materials can be obtained by fitting 10 a power-law relationship to the unloading curve using the Oliver and Pharr method. This method will be discussed in more detail in next section. However, the third type of materials with extremely high elastic recovery such as amorphous carbon nitride ($CNx$), provide a significantly curved unloading portion to such an extent that even the use of the power-law fitting relationship cannot produce an accurate measurement and consequently the extraction of mechanical properties from such a curved plot was not as straightforward as for the materials with low elastic recovery (Lu et al., 2000).





`

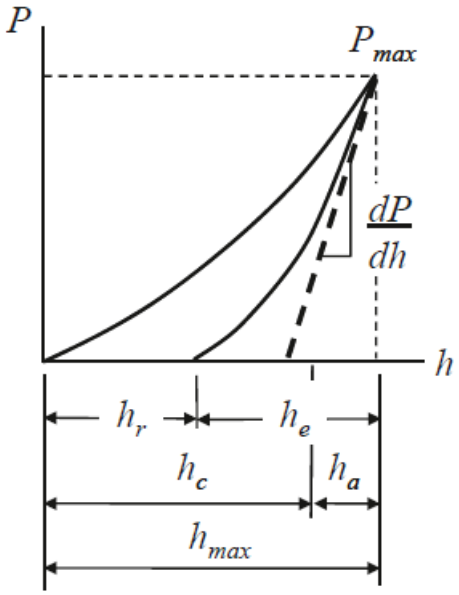


$P_{max}$ = Maximum load

$h_{max}$ = Maximum depth

$h_c$ = Depth of contact

$h_r$ = Depth of the residual impression

$h_e$ = Displacement associated with the elastic recovery during unloading

Figure 2.9: Load displacement curve (Moharrami, 2013).

Indentation elastic modulus states that elastic modulus is obtained from the slope of the tangent to calculate the indentation hardness (Hit) and is equals to the Young modulus



$$\frac{1}{E_r} = \frac{1-Vs^2}{E_{it}} + \frac{1-Vi^2}{E_i} \quad (11)$$

$E_r$: Converted elastic modulus

$E_i$: (1.14 x 1012 N/m2) Young's modulus for indenter

$Vi$ : (0.07) Poisson's ratio for indenter

$E_{it}$: Indentation elastic modulus

$Vs$: Poisson's ratio for specimen

## 2.4 Chapter summary

In this last chapter, the application of the NR in vibration isolation has been studied and elaborated. The general theories on the vibration isolation and the classes of vibration isolators were also discuss. Nanoindentation process also discuss in this chapter.





`

# CHAPTER 3

# METHODOLOGY

## 3.0 Introduction

The aim of this study is to promote SMR CV-60 as the most important substance in the development of laminated rubber metal spring (LR-MS). Prior to that, a research on transmissibility in the axial direction and parameter evaluation of LR-MS was carried out. (Salim et al., 2016). In order to investigate the compatibility of SMR CV - 60 as the main substance in LR-MS development, the hardness and the young modulus of SMR CV - 60 at various force (0.1, 0.2, 0.4, 0.6, 0.8, 1.0, 1.2, 1.4 and 1.6) $mN$ are to be investigated. This chapter will describes in details the methodologies that have been used during conducting the nanoindentation testing.





`

## 3.1 Flow Chart Project

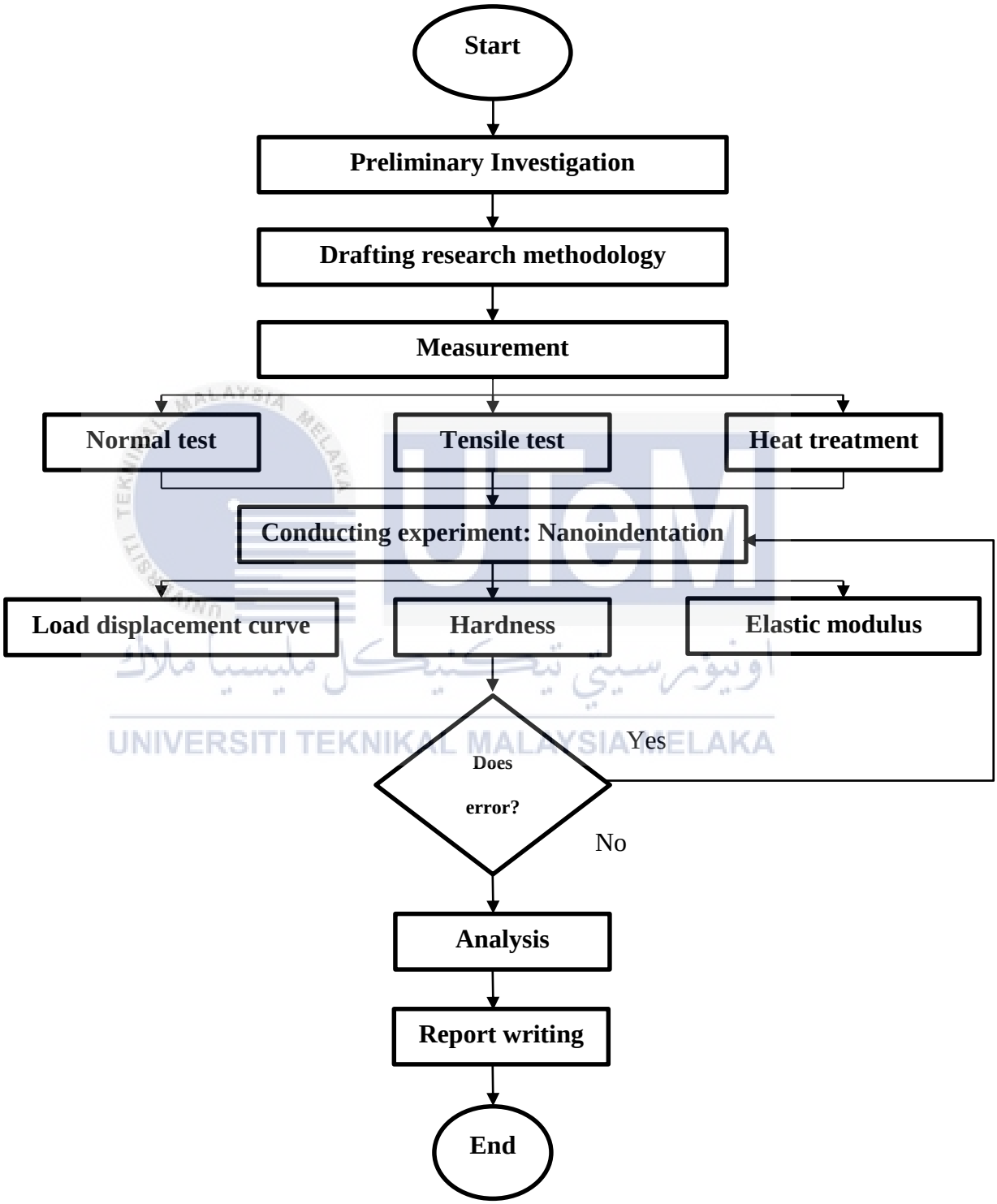


Figure 3.1: Flow chart project

`

## 3.2 Preliminary Investigation

Preliminary investigation can be said as the first step on this experiment project. Before conducting this experiment, the objectives of this project should be determined. Even the objectives should relate with the problem statement. At the beginning, the objectives are to evaluate the mechanical properties (hardness and young modulus) of SMR CV - 60 with different force ranged from (0.1, 0.2, 0.4, 0.6, 0.8, 1.0, 1.2, 1.4 and 1.6) $mN$ through nanoindentation testing and to expanding the application of the natural rubber particularly in the LR-MS development. A preliminary proposal has provided the needs in this project to let the reader knows the project plans. The details that have in the proposal are as follow.

a. Project briefing

b. Problem statement

c. Project objective

d. Project work scope

e. Project methodology

f. Result expectation

g. Reference

h. Project planning





`

## 3.3 Receiving Material

Firstly, figure 3.2 was the sample of SMR CV - 60 that was given by my supervisor Dr. Mohd Azli Bin Salim. The NR has been extensively used in various applications due to its distinctiveness over the other materials like excellent physical properties, renewable sources origins, and economical. The elasticity and flexibility of the SMR CV-60 are the main reasons for this material to be applied in various fields especially in the engineering area.

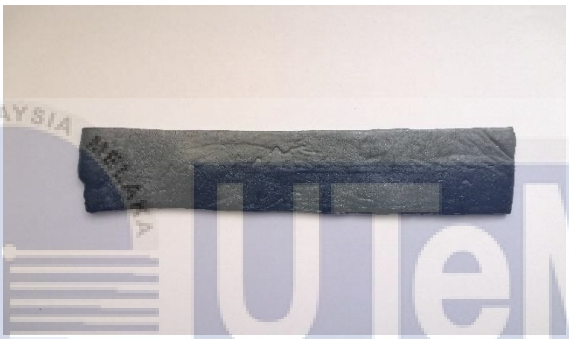

Figure 3.2: Natural rubber





`

## 3.4 Drafting Research Methodology

Drafting has been done to reduce the error while conducting the experiment. Creating a draft also helps to understand the subject in more depth and use the correct way to run experiments. Flow chart is one of the early draft have been done. Based on the draft, flow in doing this experiment become smooth





`

## 3.5 Sample Measurement

### 3.5.1 Apparatus setup for cutting NR

Figure 3.3 shown a combination of tools and material sample for carried out the cutting process of NR and figure 3.4 shown a sample has been placed into a small plastic bag after the cutting process.

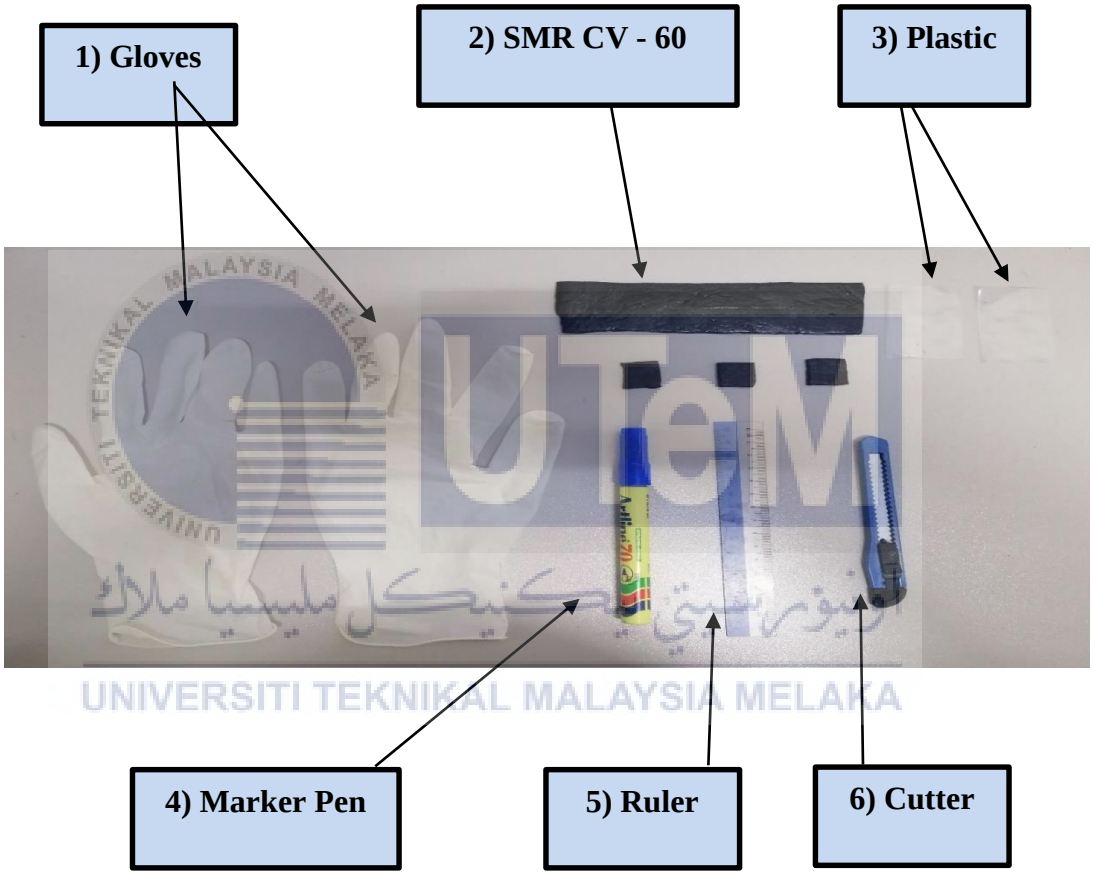




Figure 3.3: Apparatus setup for cutting NR



`

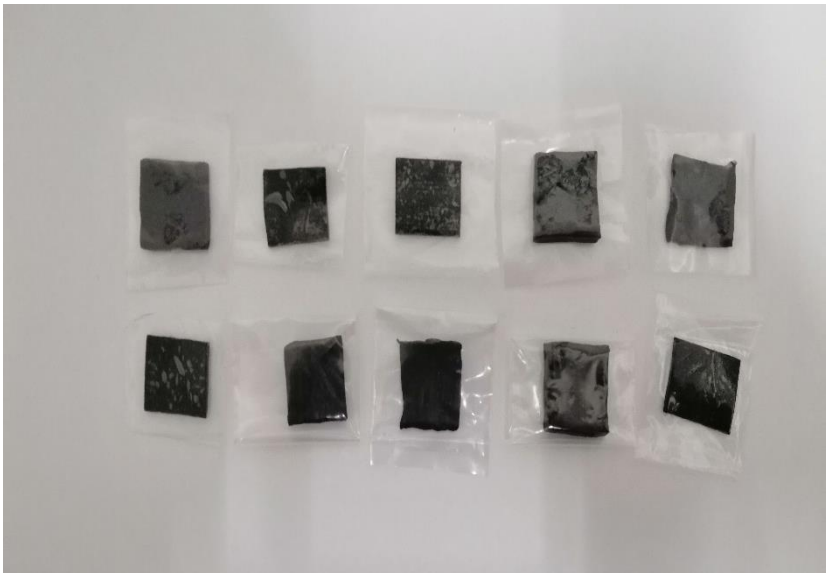

Figure 3.4: After NR cutting process

Table 3.1: Descriptions for material used

| No | Materials | Descriptions |
|---|---|---|
| 1 | Gloves | Used to prevent the surface of the sample from scratching and preventing the hands from being injured while using sharp items |
| 2 | SMR CV - 60 | Acts as a sample to be cut for this testing |
| 3 | Plastics | Used as a place for sample storage after the cutting process. This helps to keep the sample surface from being damaged |
| 4 | Marker pen | Used for marking process before cutting process |
| 5 | Ruler | Used for the marking process to be more precise |
| 6 | Cutter | Used for sample cutting process after the marking process is done |





`

### 3.5.2 Cutting SMR CV - 60 sample

Second, figure 3.5 (a) (b) shown the matrix form has been drawn on the sample surface. The matrix is drawn to determine the force placed on the sample surface which is point A(0.1 $mN$), B (0.2 $mN$), C (0.4 $mN$), D (0.6 $mN$), E (0.8 $mN$), F (1.0 $mN$), G (1.2 $mN$), H (1.4 $mN$) and I (1.6 $mN$). The "X" symbol refer to the point on the sample surface that need to be applied force. This helps to compare the force result between each sample which is sample 1 until sample 10.

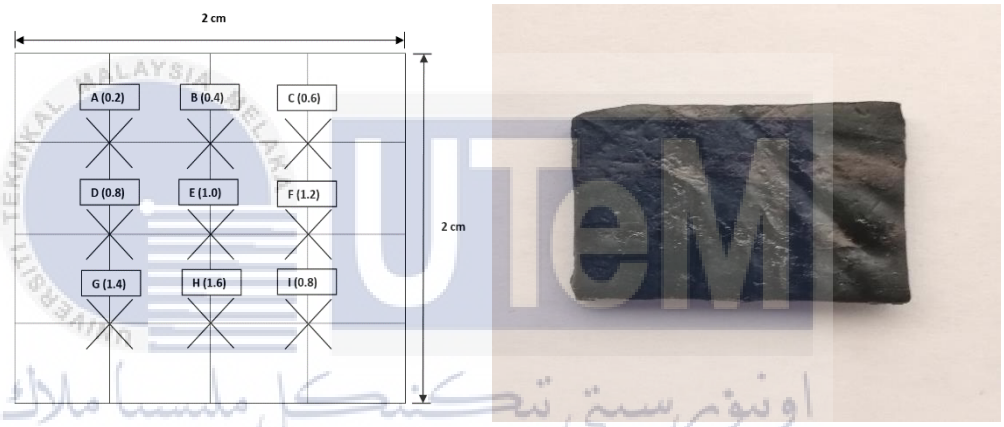


(a) (b)



Figure 3.5: NR (a) matrix drawing, (b) matrix drawing on surface sample of NR



`

## 3.6 SMR CV – 60 condition before nanoindentation test

### 3.6.1 Normal test

Normal test refers to a situation where the sample SMR CV-60 is in its original state without going through any test before making a nanoindentation test to obtain hardness and young modulus. Its refer to sample 1 and sample 2

### 3.6.2 Tensile test

Tensile test have been carried out to the sample 3 ,4, 5, 6, 7 and 8 after cutting process. This test carried out before the nanoindentation test in order to compare the original sample and after sample have been stretch. Figure 3.6 shown the orientation of stretching sample which is only at Y-axis without any torsion. Figure shown tensile machine used which is SHIMA Universal Material Testing. After tensile test, the SMR CV-60 will elongate and change in shape. Then, the sample hardness and young modulus will be test again using nanoindentation test.



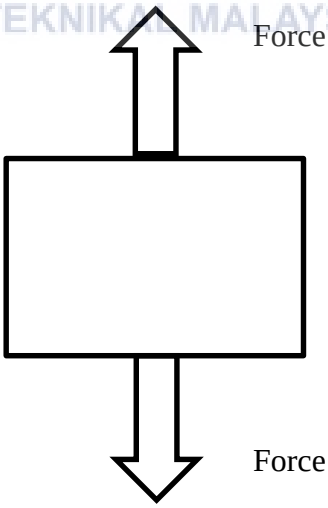


Figure 3.6: Orientation of stretching sample



`

Table 3.2: Sample and rate of tensile test

| No | Sample | Tensile test (mm/min) |
|---|---|---|
| 1 | 3 and 4 | 100 |
| 2 | 5 and 6 | 200 |
| 3 | 7 and 8 | 300 |

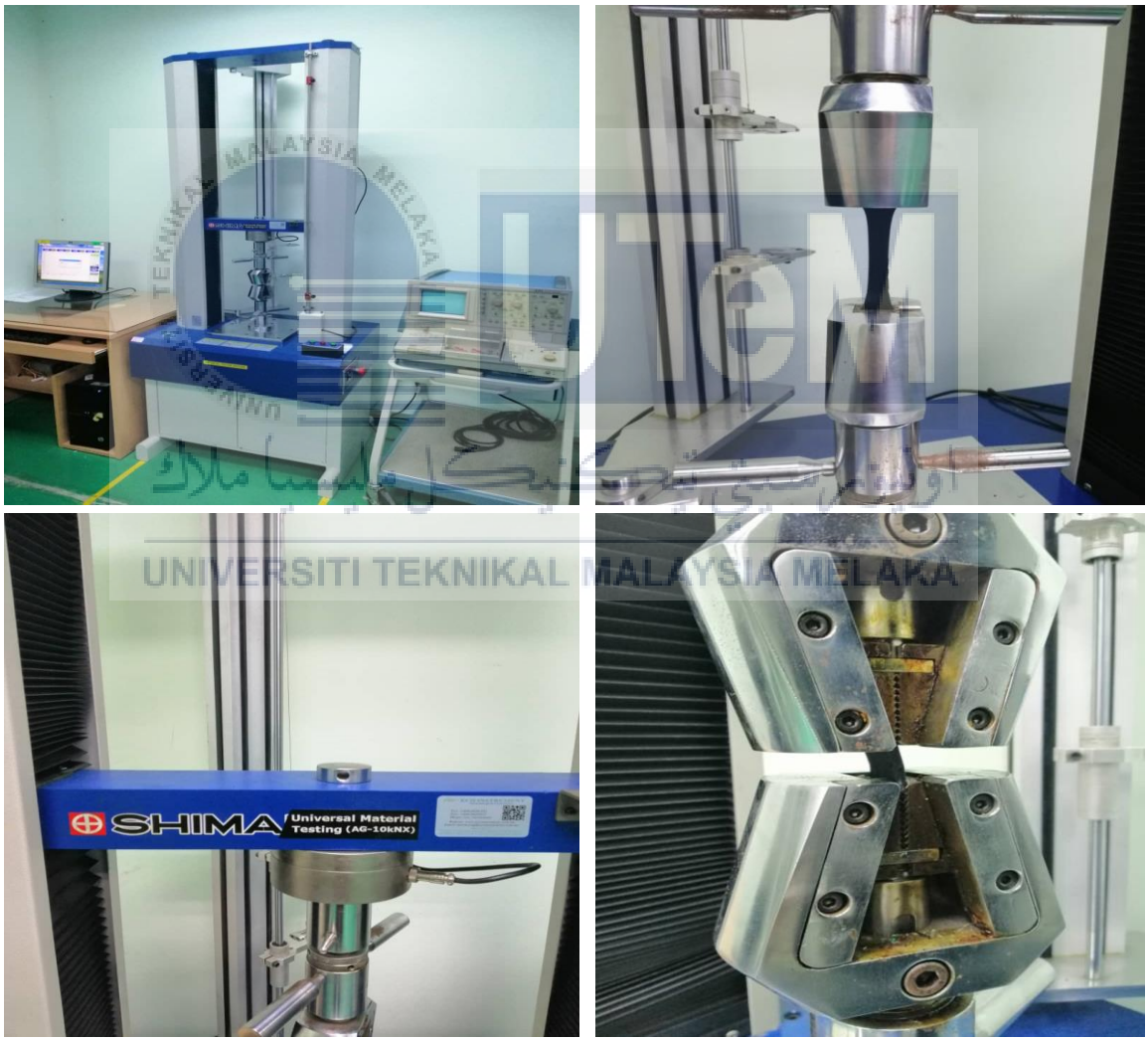


Figure 3.7: SHIMA Universal Material Testing



`

### 3.6.3 Heat treatment

Heat treatment is a process in which a metal is heated to a certain temperature and the cooled in a particular manner to alter its internal structure for obtaining desired degree of physical and mechanical properties such as brittleness, hardness, and softness. Heat treatment have been done on samples 9 and 10 after cutting process. Sample 9 is subject to a temperature of 100 and 150 for sample 10. Both sample exposed to heat at 1 hour. After that, sample will be cool down first before starting the nanoindentation test to obtain hardness and young modulus. Figure shown machine used to do a heat treatment

Table 3.3: Sample and value of heat treatment

| No | Sample | Heat treatment (℃) |
|---|---|---|
| 1 | 9 | 100 |
| 2 | 10 | 150 |





`


Figure 3.8: Oven

## 3.7 Nanoindentation Testing

The indentation testing was used to determine the strength properties of materials through its surface. This testing was conducted to measure the SMR CV-60 hardness and young modulus. The study of hardness and young modulus testing was carried out by using a nano-hardness tester, Shimadzu Dynamic Ultra Micro Hardness Tester Model DUH-211 as shown in figure 3.9. The nano-indenter type was equipped with an imaging device that capable to switch back and forth from the optical microscope to the indenter tips. The mounted imaging device helps to identify accurately the desirable indentation point. A standard 115 degree triangular pyramidal indenter, the Berkovich type was used in this study.





`


Figure 3.9: Shimadzu nano - hardness tester

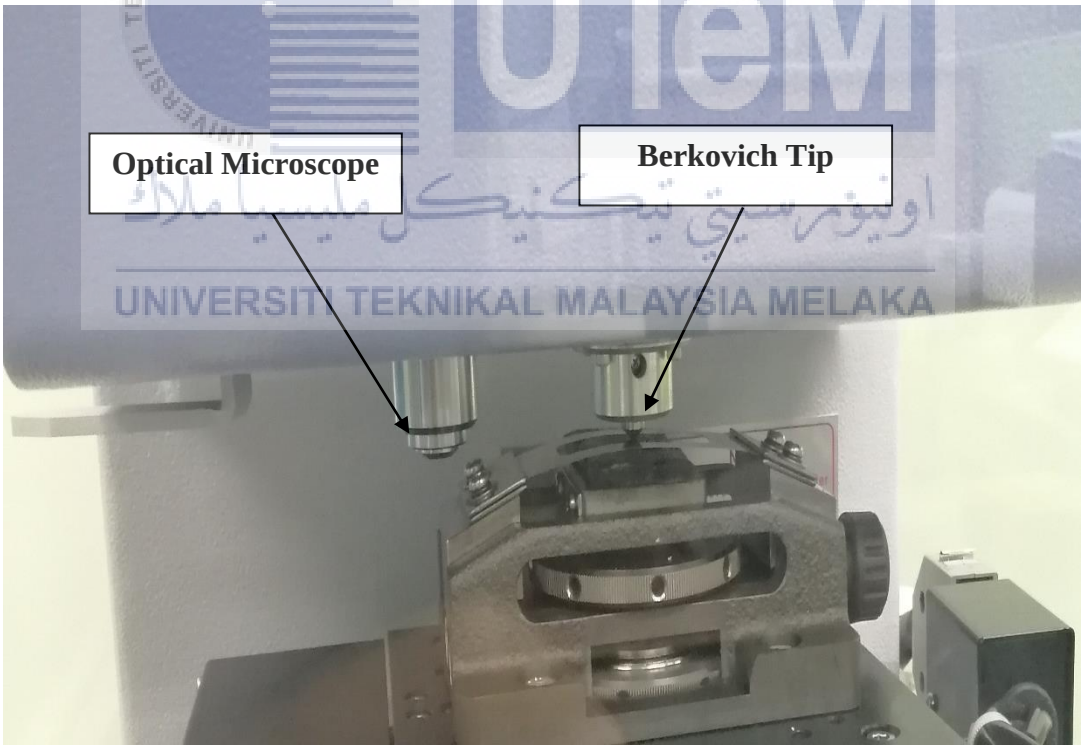


Figure 3.10: Optical microscope and Berkovich tip for Shimadzu nano - hardness tester





`

### 3.7.1 Hardness and young modulus testing

Firstly, the test piece which is SMR CV-60 sample was placed under an optical microscope to determine the indentation point. Optical microscopic is equipped with lamps to see the samples more clearly. Through optical microscope, we can see the structure of NR more clearly, so we can determine the indentation point more accurate. After that, the platform was moved to the indenter side. Testing were performed under the ambient temperature of 24 ℃. The load – hold – unload was conducted on 10 sample which is each sample will have point A (0.1 $mN$), B (0.2 $mN$), C (0.4 $mN$), D (0.6 $mN$), E (0.8 $mN$), F (1.0 $mN$), G (1.2 $mN$), H (1.4 $mN$) and I (1.6 $mN$). The loading speed have been set, which is 0.0150 $mN$/sec). The machine was fully operated with the aid of DUH211 software. Figure 3.11 (a) (b) shown while using DUH211 software to obtain hardness and young modulus result. After start the testing, each point of sample takes 5 -7 minutes to obtain the result, so that mean 1 sample takes 45 – 50 minutes because 1 sample will have 9 point to be tested. This software will generate the result in excel form.



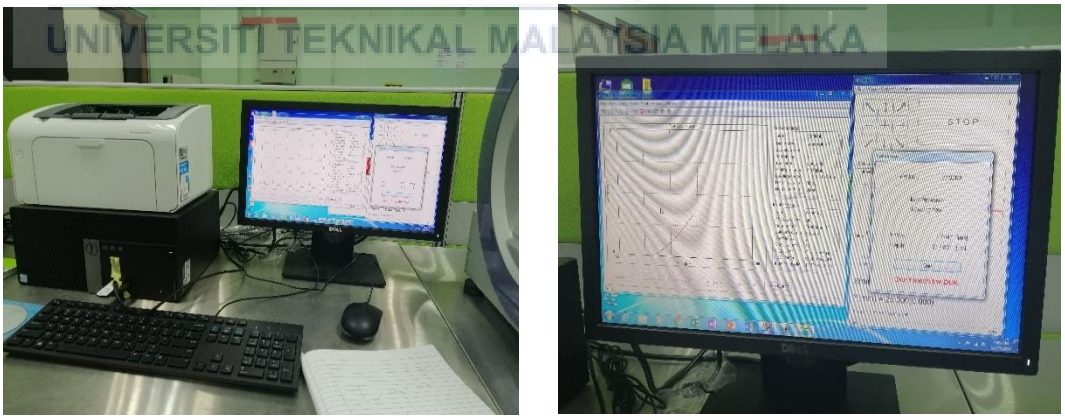

(a) (b)

Figure 3.11: (a) (b) DUH211 software setup



`

### 3.7.2 Load displacement graph plotting

Nanoindentation load-displacement curves (often known as P-h or P-δ curves) are the materials response reflected in the continuous measurement of the depth of penetration while the load is increasing from zero to the maximum load (loading curve) and then decreasing from maximum load to zero (unloading curve). After the sample was mounted on the platform, "start test" button will be click on the software. The software will generate result in form of raw data which is force and depth. Figure 3.10 represent raw data obtain from DUH211 software. Based on the raw data, load displacement need to be plotted. Origin 8 software was used to plot the data. Origin 8 provides scientists and engineers with a data analysis and a graphics workspace. New features include multi-sheet workbooks with spark lines, increased import capabilities, SQL queries, automatic analysis results recalculation and new types of graphs. Figure shown while using Origin 8 to plot the load displacement curve. Once completing the experiment, data have been collected and analysed thoroughly.





`

### 3.8 Expected table for result

a) Normal test (Sample 1 and sample 2)

Table 3.4: Sample 1 and 2 expected table

| | **Sample 1** | | **Sample 2** | |
|---|---|---|---|---|
| **Point ($mN$)** | **Hardness ($HV$)** | **Young Modulus ($N/mm2$)** | **Hardness ($HV$)** | **Young Modulus ($N/mm2$)** |
| A (0.1) | | | | |
| B(0.2) | | | | |
| C(0.4) | | | | |
| D(0.6) | | | | |
| E(0.8) | | | | |
| F(1.0) | | | | |
| G(1.2) | | | | |
| H(1.4) | | | | |
| I(1.6) | | | | |





`

b) Tensile test (Sample 3, 4, 5, 6, 7 and 8)

**Table 3.5:** Sample 3, 4, 5, 6, 7 and 8 expected table

| | **Sample 3** | | | | **Sample 4** | | | |
|---|---|---|---|---|---|---|---|---|
| **Point ($mN$)** | **Hardness ($HV$)** | | **Young Modulus ($N/mm2$)** | | **Hardness ($HV$)** | | **Young Modulus ($N/mm2$)** | |
| | **Before Tensile Test** | **After Tensile Test** | **Before Tensile Test** | **After Tensile Test** | **Before Tensile Test** | **After Tensile Test** | **Before Tensile Test** | **After Tensile Test** |
| A(0.1) | | | | | | | | |
| B(0.2) | | | | | | | | |
| C(0.4) | | | | | | | | |
| D(0.6) | | | | | | | | |
| E(0.8) | | | | | | | | |
| F(1.0) | | | | | | | | |
| G(1.2) | | | | | | | | |
| H(1.4) | | | | | | | | |
| I(1.6) | | | | | | | | |





`

c) Heat treatment (Sample 9 and 10)

Table 3.6: Sample 9 and 10 expected table

| Point ($mN$) | Sample 9 | | | | Sample 10 | | | |
|---|---|---|---|---|---|---|---|---|
| | Hardness ($HV$) | | Young Modulus ($N/mm2$) | | Hardness ($HV$) | | Young Modulus ($N/mm2$) | |
| | Before Heat | After Heat | Before Heat | After Heat | Before Heat | After Heat | Before Heat | After Heat |
| A (0.1) | | | | | | | | |
| B(0.2) | | | | | | | | |
| C(0.4) | | | | | | | | |
| D(0.6) | | | | | | | | |
| E(0.8) | | | | | | | | |
| F(1.0) | | | | | | | | |
| G(1.2) | | | | | | | | |
| H(1.4) | | | | | | | | |
| I(1.6) | | | | | | | | |



## 3.9 Chapter summary



All methodologies used in this study were presented in this chapter. One types of NR compound supplied by the supervisor were used in this study which is SMR CV-60. In order to achieve this objective, a nanoindentation test was conducted to obtained mechanical properties for NR which is SMR CV-60 in 3 different types of NR conditions which is normal test, tensile test and heat treatment with different force which is 0.1, 0.2, 0.4, 0.6, 0.8, 1.0, 1.2, 1.4 and 1.6 $mN$.



`

# CHAPTER 4

# RESULT AND DISCUSSION

## 4.0 Introduction

In this chapter, all the data obtained from the experiment are presented and discussed more thoroughly. In order to achieve this objective, a nanoindentation test was conducted to obtained mechanical properties for NR which is SMR CV-60 in 3 different types of NR conditions which is normal test, tensile test and heat treatment with different force which is 0.1, 0.2, 0.4, 0.6, 0.8, 1.0, 1.2, 1.4 and $1.6mN$. Through the nanoindentation test, (hardness and young modulus) for 3 different types of NR conditions which is normal test, tensile test and heat treatment with different force were recorded and analyzed. The compatibility of the SMR CV-60 as the main materials in the development of LR-MS was also discussed.





`

## 4.1 Nanoindentation result

### 4.1.1 Normal test (Sample 1 and 2)

Table 4.1: Hardness and young modulus for normal test

| | Sample 1 | | Sample 2 | |
|---|---|---|---|---|
| **Point ($mN$)** | **Hardness ($HV$)** | **Young Modulus ($N/mm2$)** | **Hardness ($HV$)** | **Young Modulus ($N/mm2$)** |
| A (0.1) | 0.019 | 6.485 | 0.017 | 6.521 |
| B(0.2) | 0.02 | 6.671 | 0.02 | 6.671 |
| C(0.4) | 0.022 | 6.8208 | 0.023 | 6.734 |
| D(0.6) | 0.03 | 6.909 | 0.028 | 6.909 |
| E(0.8) | 0.036 | 8.948 | 0.037 | 8.948 |
| F(1.0) | 0.034 | 8.634 | 0.034 | 7.634 |
| G(1.2) | 0.026 | 8.11 | 0.027 | 7.21 |
| H(1.4) | 0.025 | 8.036 | 0.026 | 7.022 |
| I(1.6) | 0.025 | 8.046 | 0.025 | 7.212 |





`

a) Load displacement curve

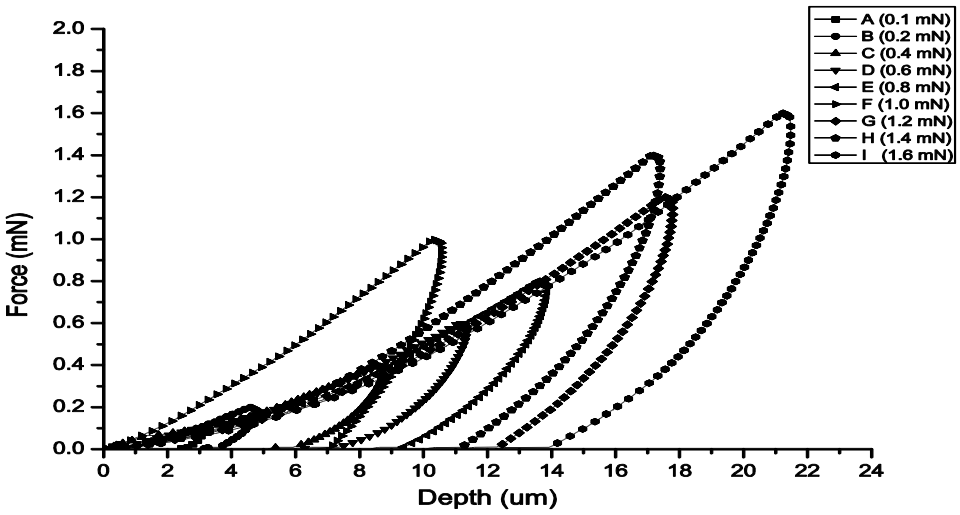


**(a)**

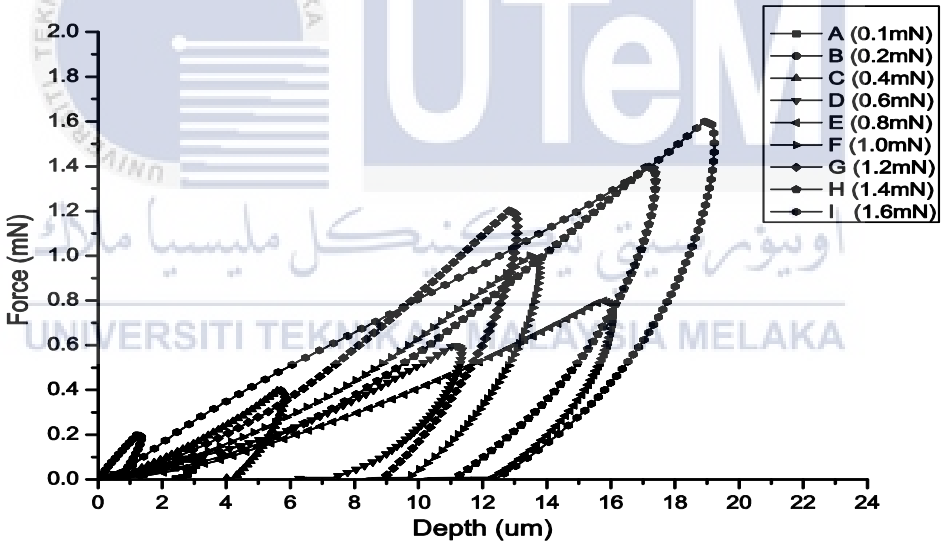


(b)

Figure 4.1: Graph load displacement curve (a) sample 1 (b) sample 2





`

The increasing of penetration depth, $hmax$ with the increasing the force applied (0.1, 0.2, 0.4, 0.6, 0.8, 1.0, 1.2, 1.4, 1.6) $mN$ was showed that the properties of the vulcanized SMR CV -60 were influenced by the amount of forced applied. The influenced of force applied by the indenter in the SMR CV -60 was showed with the variation of viscous – elastic to elastic – plastic deformation modes that observed in force – indentation depth curves for SMR CV -60. Figure 4.1 shown that the remnant depth values were slightly dependent on the forces applied. The typical loading – unloading curves of forces versus penetration depth for SMR CV-60 at different force were plotted separately in Figure 4.1. The curves have showed that the compounds have exhibited for different deformation modes depending on the force applied. Together with that, based on the figures, it was showed the remnant depth at the end of the unloading curve were randomly varies from 2.4176 to 12.2373 for both sample.





`

b) Hardness

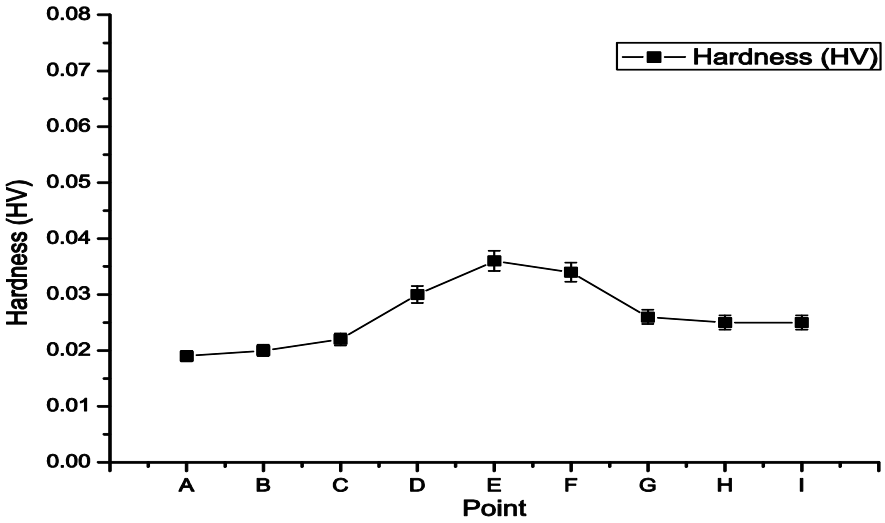


(a)

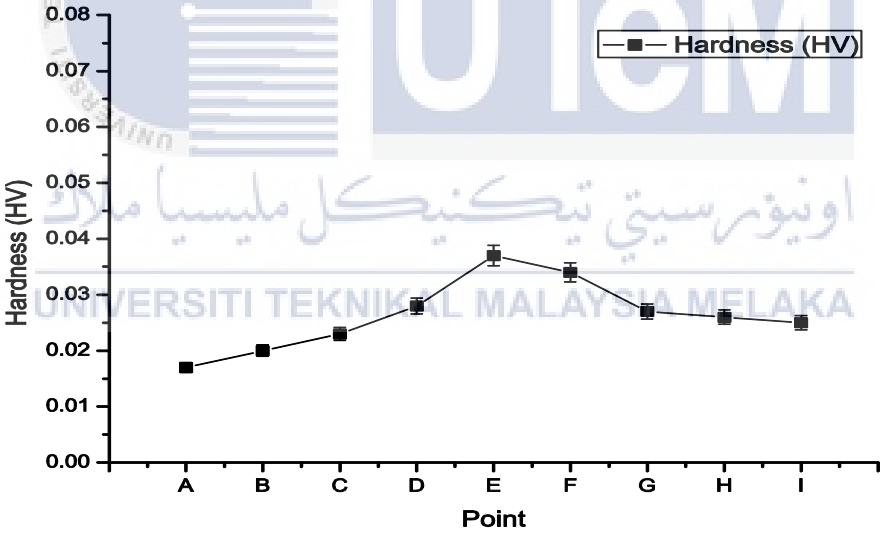


(b)

Figure 4.2: Graph hardness (a) sample 1 (b) sample 2





`

The relationship between the material hardness with the different force applied for sample 1 and sample 2 has been presented in Figure 4.2. Sample 1 and sample 2 were the same normal tests which hardness and young modulus will be obtained using the nanoindentation method. The main reason for using two samples for one purpose is to reinforce the results obtained. Sample 1 and sample 2 are undifferentiated from each other, as the graph showed a same trend which are increasing trend from point A to point B. The hardness values obtained each time for the same specimen are slightly differences. Their differences may due to the grains, grain boundaries, defects and impurities of surface of the specimen (The & One, n.d.). The different is very small actually which is in Nano scale. The hardness value for point A ($0.1mN$) are 0.019 for sample 1 and 0.038 $mN$ for sample 2. Based on the graph above, the hardness was slightly increase from point A (0.1 $mN$) to point C (0.4 $mN$) for both sample with the value of 0.019 $mN$ to 0.022 $mN$ for sample 1 and 0.017 to 0.023. Then, there was a gradually increase at point C (0.4 $mN$) to E (0.8 $mN$) for both sample with the value of 0.022 to 0.036 for sample 1 and sample 2. The hardness value was found to be decreasing starting from point F(1.0 $mN$) to the last point which is point I(1.6 $mN$) with a value of 0.034 to 0.025 for sample 1 and 0.034 to 0.025 for sample 2. The main reason why the hardness only increase slightly from point A to point B were because of point position. As we can see on the figure, the position of point A, B and C located at the top of the sample, so, actually in the beginning of the study, the sample was cut using scissors. Force will be applied to each side of the sample. Therefore, the adjacent point will feel the change in terms of thickness, shape and structure of SMR CV -60 while point E is located at the center/centriod of the sample which does not feel much change on the structure which makes the hardness higher than





`

the other point that near the sample side. Their differences in hardness value may be due to the grains, grain boundaries, defects and impurities of surface of the specimen (The & One, n.d.).





`

c) Young modulus

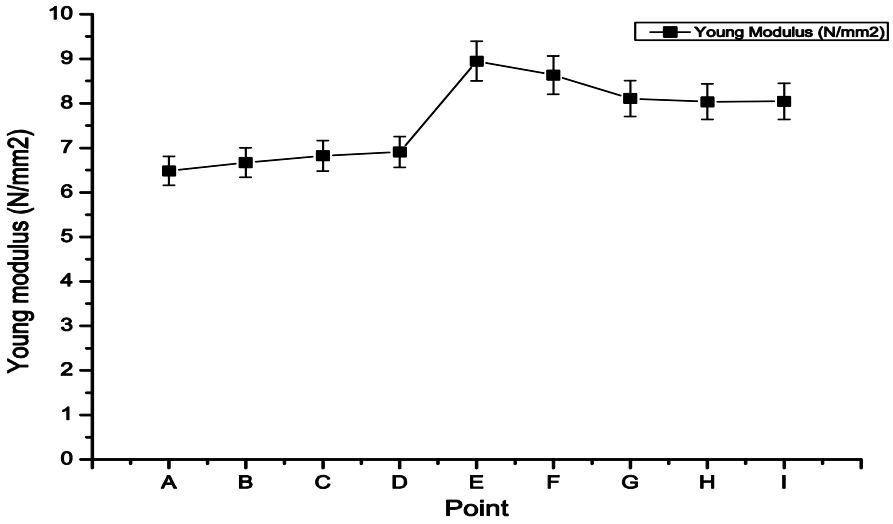


(a)

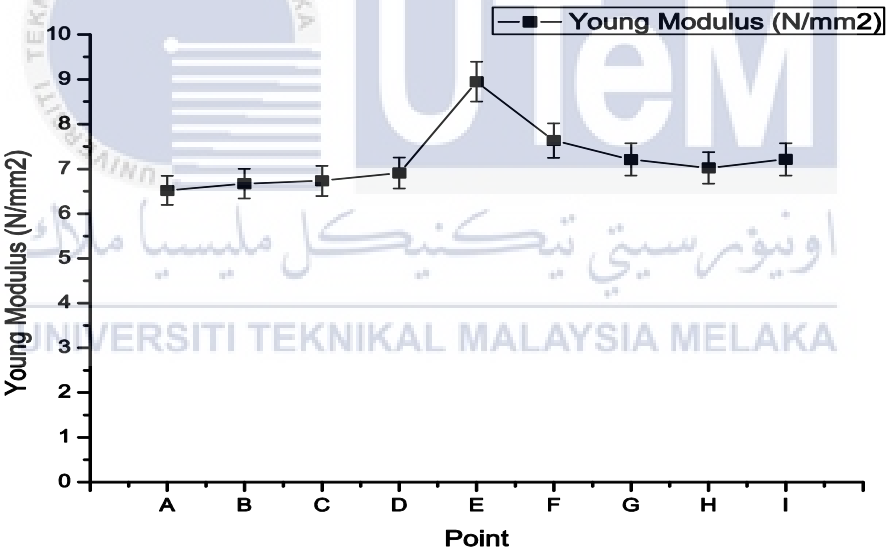


(b)

Figure 4.3: Graph young modulus (a) sample 1, (b) sample 2





`

The recorded Young modulus at different force for sample 1 and sample 2 was plotted separately in figure 4.3. Sample 1 and sample 2 are undifferentiated from each other, as the graph showed a same trend which are increasing trend from point A to point B. As shown in Figure 4.3, the elastic modulus for both sample was found to be increase from point A (0.1 $mN$) to point I (1.6 $mN$) which are 6.485 to 8.046 for sample 1 and 6.521 to 7.212. Based on the graph above, the hardness was slightly increase from point A (0.1 $mN$) to point D (0.6 $mN$) for both sample with the value of 6.485 to 6.909 for sample 1 and 6.521 to 7.212 for sample 2. There was a sudden increase from point D to E point which is 6.909 to8.948 for sample 1 and 6.909 to 8.948 for sample 2. From point F to point I, young modulus slightly decrease which is 8.634 to 8.046 for sample 1 and 7.634 to 7.212 for sample 2. Rubber is a unique material that is both elastic and viscous. Rubber parts can therefore function as shock and vibration isolators and/or as dampers. Rubber has a low modulus of elasticity and is capable of sustaining a deformation of as much as 1000 percent (Schaefer, n.d.). The value of young modulus are different from point A to point I because Young's modulus is meaningful only in the range in which the stress is proportional to the strain, and the material returns to its original dimensions when the external force is removed. As stresses increase, Young's modulus may no longer remain constant but decrease, or the material may either flow, undergoing permanent deformation, or finally break The main reason why the young modulus only increase slightly from point A to point C were same explanation as hardness value because of point position. As we can see on the figure, the position of point A, B and C located at the top of the sample





`

### 4.1.2 Tensile test (100 mm/min)

Table 4.2: Hardness and young modulus for tensile test (100 mm/min)

| Point ($mN$) | Sample 3 | | | | Sample 4 | | | |
|---|---|---|---|---|---|---|---|---|
| | Hardness ($HV$) | | Young Modulus ($N/mm2$) | | Hardness ($HV$) | | Young Modulus ($N/mm2$) | |
| | Before Tensile Test | After Tensile Test | Before Tensile Test | After Tensile Test | Before Tensile Test | After Tensile Test | Before Tensile Test | After Tensile Test |
| A(0.1) | 0.018 | 0.02 | 4.745 | 3.745 | 0.022 | 0.02 | 4.745 | 3.555 |
| B(0.2) | 0.02 | 0.018 | 5.145 | 4.145 | 0.024 | 0.022 | 5.145 | 4.171 |
| C(0.4) | 0.022 | 0.022 | 5.121 | 4.121 | 0.026 | 0.025 | 5.643 | 4.56408 |
| D(0.6) | 0.022 | 0.02 | 5.58 | 5.022 | 0.026 | 0.026 | 5.815 | 5.409 |
| E(0.8) | 0.03 | 0.028 | 7.835 | 7.233 | 0.03 | 0.028 | 7.22 | 7.048 |
| F(1.0) | 0.022 | 0.016 | 6.835 | 6.433 | 0.028 | 0.026 | 6.65 | 6.334 |
| G(1.2) | 0.021 | 0.019 | 5.724 | 4.724 | 0.027 | 0.025 | 5.724 | 4.81 |
| H(1.4) | 0.017 | 0.015 | 5.468 | 4.468 | 0.024 | 0.024 | 5.468 | 4.536 |
| I(1.6) | 0.017 | 0.015 | 5.468 | 4.468 | 0.023 | 0.022 | 5.223 | 4.41 |





`

a) Load displacement curve (Tensile at 100 mm/min)

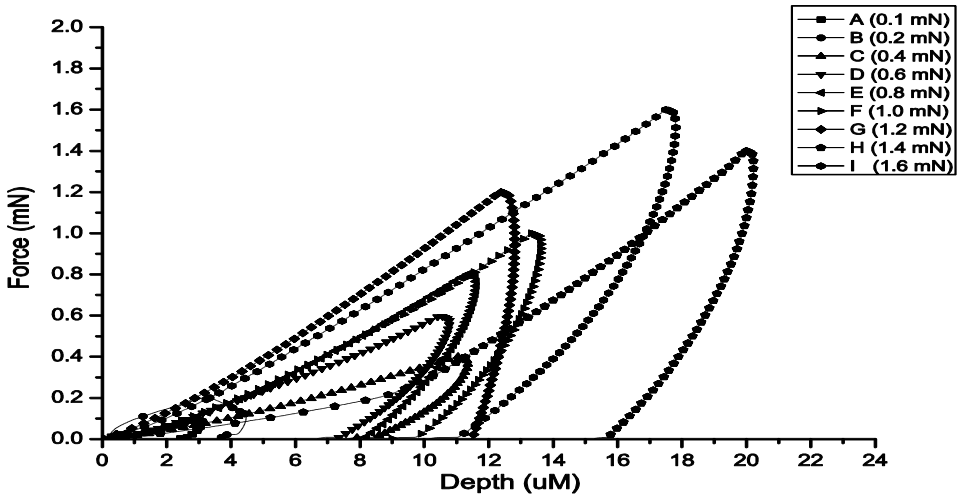


(a)

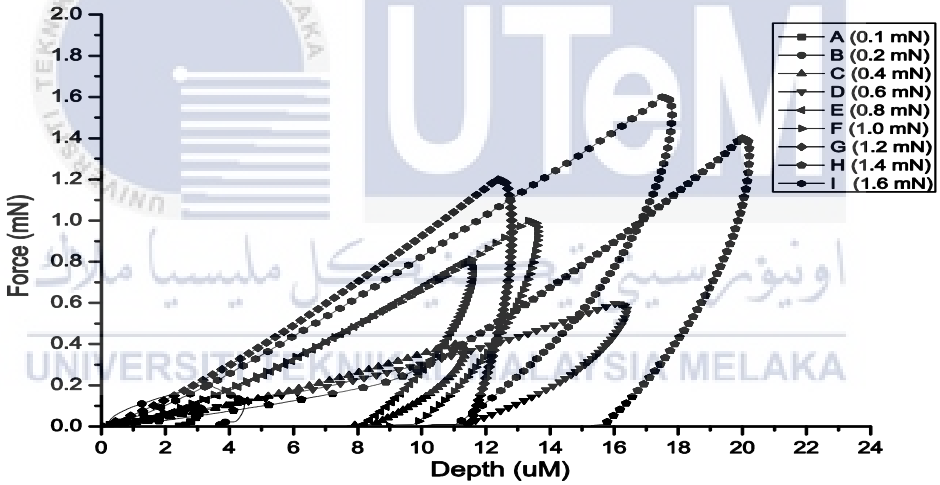


(b)

Figure 4.4: Graph load displacement curve (a) sample 3 (b) sample 4

As shown in figure 4.4, the curves have showed that the compounds have exhibited for different deformation modes depending on the force applied. Together with that, based on the figures, it was showed the remnant depth at the end of the unloading curve were randomly varies from 2.4176 to 19.86 for both sample.



`

b) Hardness

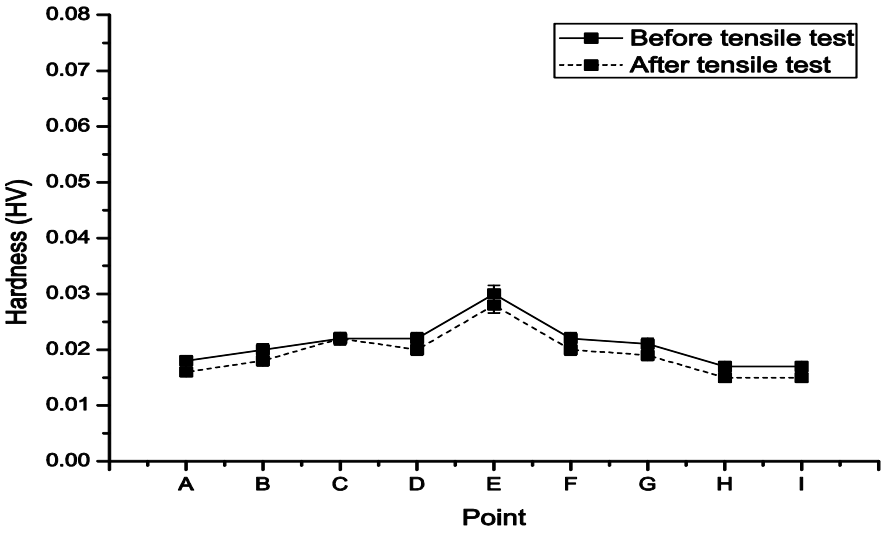


(a)

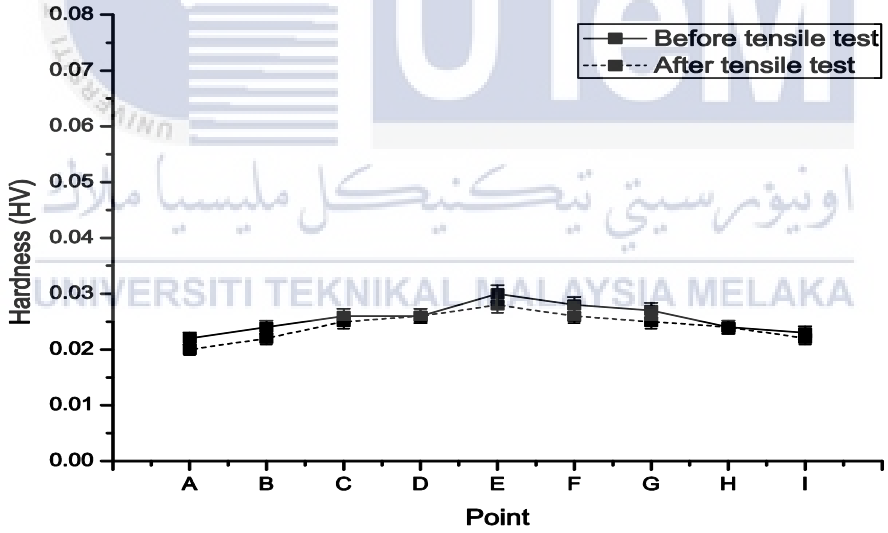


(b)

Figure 4.5: Graph hardness for (a) sample 3, (b) sample 4





`

The recorded hardness (before and after tensile test) at different force for sample 3 and sample 4 was plotted separately in figure 4.5. For Sample 3 and 4, tensile test (100 mm/min) have been done to the NR and the data collected before and after test have been plotted and compared. The correlation between the material hardness with the force applied for SMR CV-60 has been presented in figure above. The graph showed that hardness value of SMR CV-60 for before and after tensile test is unpredictable with force from 0.1 $mN$ to 1.6 $mN$. There is no major gap for hardness value between before and after tensile test. Based on both graph, we can see a same trend between sample 1 and sample 2. As shown in figure, for overall, we can see that the hardness decrease after tensile test 100 mm/min. For both sample was found slightly increase from point A to point I which is 0.018 to 0.023 and hardness (after tensile test) for sample 3 was slightly decrease from 0.02 to 0.015 while for sample 4, increase from 0.02 to 0.022. The change in hardness value is not too much because the force applied is only 100 mm / min. As we can see at point E for sample 3 and point D for sample, the hardness value remain unchanged. The main reason why hardness remain unchanged is less deformation at point C compare to point A and B where its related with the statement saying that Rubber has elastic properties similar to those of a metallic spring and has energy absorbing properties and these viscoelastic properties allow rubber to maintain a constant shape after deformation, while simultaneously absorbing mechanical energy (Schaefer, n.d.)





`

c) Young modulus

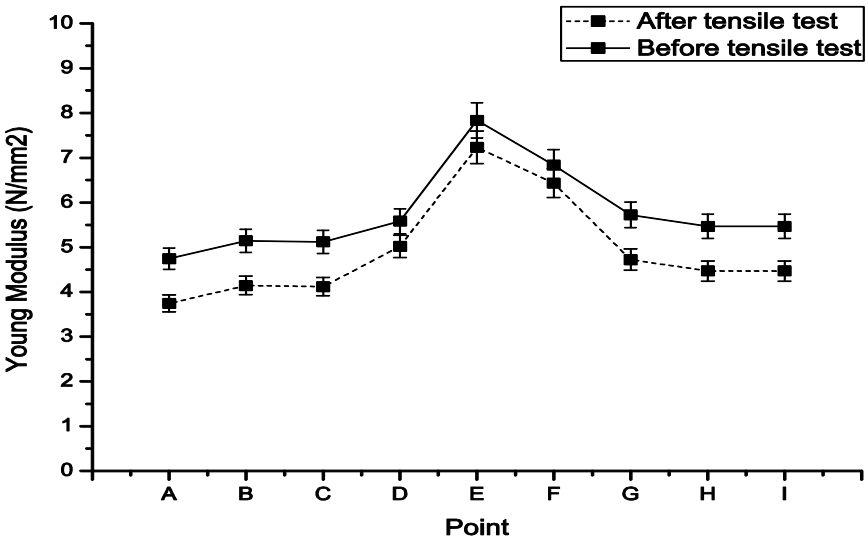


(a)

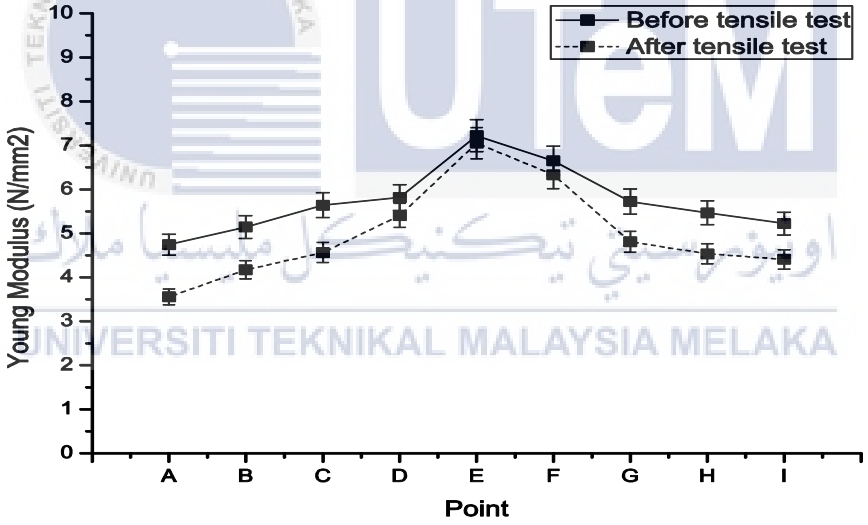


(b)

Figure 4.6: Graph young modulus (a) sample 3 (b) sample 4





`

The obtain results for elastic modulus (before and after tensile test) at different force for sample 3 and sample 4 was plotted separately in figure 4.6. Tensile test at 100 mm/min have been done to the NR to see the differences between before and after tensile test. The young modulus value for before and after tensile test was slightly change as the force increase. As we can see based on the graph above, the value of elastic modulus for before tensile test is higher than after tensile test. As shown in Figure 4.6 (a), the elastic modulus (before tensile test) for sample 3 was found to be slightly decrease from 4.745 to 5.468 and elastic modulus (after tensile test) for sample 3 was also increase from 3.745 to 4.468. Meanwhile, the elastic modulus (before tensile test) range for sample 4 was found increase from 4.745 to 5.223 and elastic modulus (after tensile test) for sample 4 was also increase from 3.555 to 4.41. For overall, we can see that the young modulus decrease after tensile test 100 mm/min where its related with the statement saying that as stresses increase, Young's modulus may no longer remain constant but decrease, or the material may either flow, undergoing permanent deformation, or finally break (Young & Young, 2019). Small gap between this two graphs have been noticed. In addition, Figure 4.6 (a)(b), much gap between before and after tensile test at point A, B, C, G, H and I. This happen because of point position. Point A, B, C located at top of the SMR CV 60 where it located near the tensile test clamp. Surely it will experience much force compare to point D, E and F which located at the middle of sample.





`

### 4.1.3 Tensile test (200 mm/min)

Table 4.3: Hardness and young modulus for tensile test (200 mm/min)

| Point ($mN$) | Sample 5 | | | | Sample 6 | | | |
|---|---|---|---|---|---|---|---|---|
| | Hardness ($HV$) | | Young Modulus ($N/mm2$) | | Hardness ($HV$) | | Young Modulus ($N/mm2$) | |
| | Before Tensile Test | After Tensile Test | Before Tensile Test | After Tensile Test | Before Tensile Test | After Tensile Test | Before Tensile Test | After Tensile Test |
| A(0.1) | 0.023 | 0.018 | 4.545 | 3.121 | 0.026 | 0.02 | 4.365 | 3.224 |
| B(0.2) | 0.025 | 0.02 | 5.231 | 3.345 | 0.027 | 0.021 | 5.143 | 3.575 |
| C(0.4) | 0.028 | 0.024 | 5.374 | 3.521 | 0.028 | 0.021 | 5.332 | 3.665 |
| D(0.6) | 0.03 | 0.028 | 5.88 | 4.822 | 0.031 | 0.029 | 5.766 | 5.014 |
| E(0.8) | 0.036 | 0.033 | 7.677 | 6.533 | 0.039 | 0.037 | 7.722 | 6.787 |
| F(1.0) | 0.03 | 0.027 | 6.413 | 5.33 | 0.035 | 0.032 | 6.656 | 5.45 |
| G(1.2) | 0.029 | 0.025 | 5.755 | 3.924 | 0.029 | 0.0223 | 5.899 | 3.768 |
| H(1.4) | 0.03 | 0.024 | 5.566 | 3.768 | 0.028 | 0.023 | 5.423 | 3.412 |
| I(1.6) | 0.03 | 0.024 | 5.433 | 3.668 | 0.027 | 0.021 | 5.575 | 3.568 |





`

a) Load displacement curve (Sample 5 and sample 6)

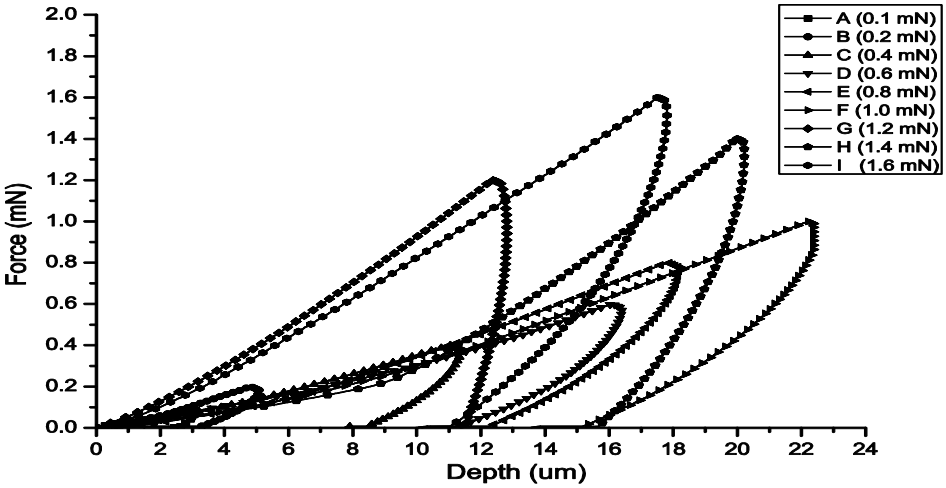


(a)

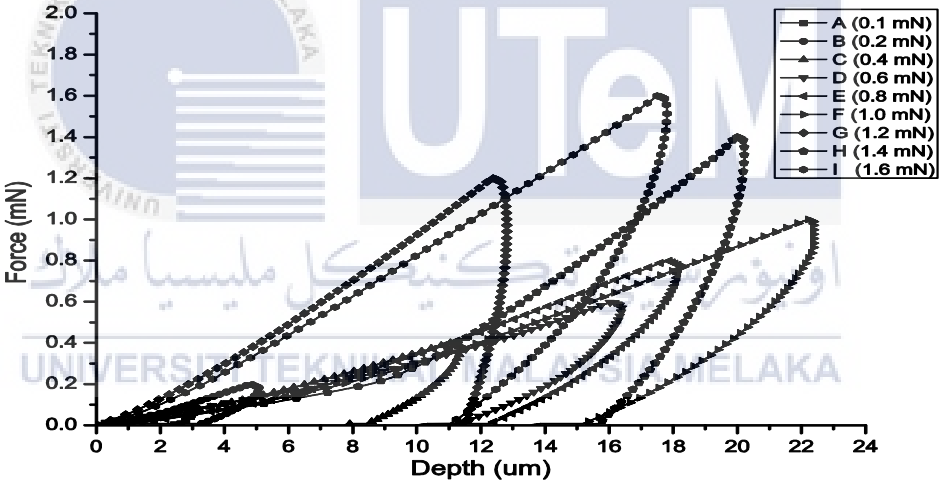


(b)

Figure 4.7: Graph load displacement curve (a) sample 5 (b) sample 6

As shown in figure 4.7, the curves have showed that the compounds have exhibited for different deformation modes depending on the force applied. Together with that, based on the figures, it was showed the remnant depth at the end of the unloading curve were randomly varies from 2.1433 to 15.798 for both sample.



`

b) Hardness

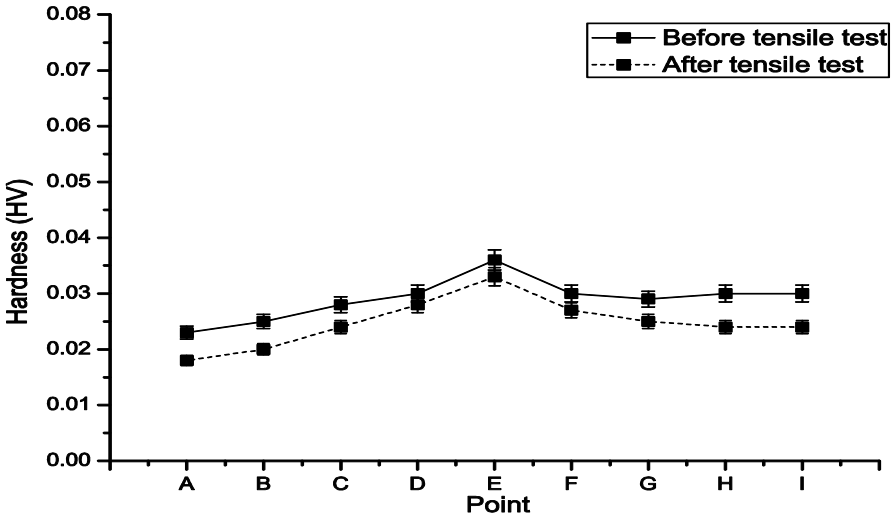


(a)

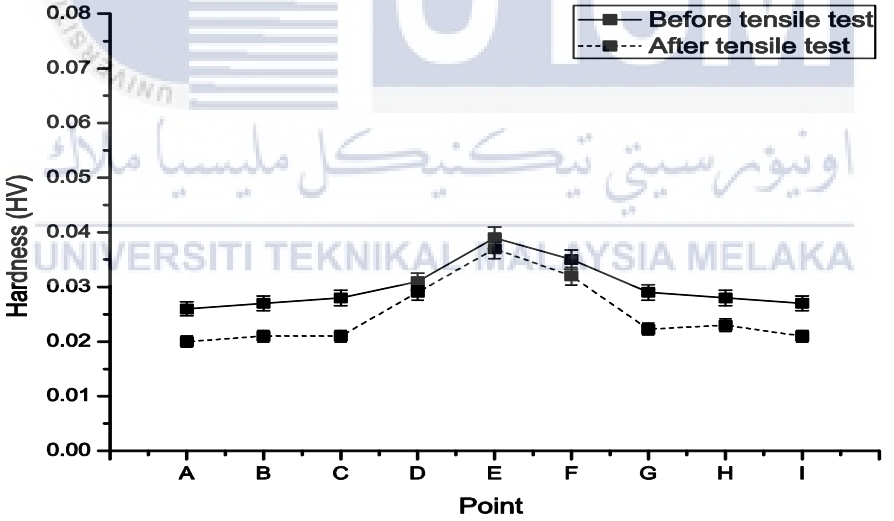


(b)

Figure 4.8: Graph hardness (a) sample 5 (b) sample 6





`

Hardness (before and after tensile test) at different force for sample 5 and sample 6 was plotted separately in figure 4.8. For Sample 5 and 6, tensile test (200 mm/min) have been done to the SMR CV-60 and the data collected before and after test have been plotted and compared. The graph showed that hardness value of SMR CV-60 for before and after tensile test is unpredictable with force from 0.1 $mN$ to 1.6 $mN$. The graph started to show a gap for hardness value after tensile compare to previous sample 3 and 4, which the gap still cannot be seen clearly. Based on the both graph, we can see a same trend between sample 5 and sample 6. For overall, we can see that the hardness decrease after tensile test 200 mm/min. For both sample was found slightly increase from point A to point I which is 0.023 to 0.030 and hardness (after tensile test) for sample 5 was also increase from 0.018 to 0.024 while sample 6 also shown increasing trend. The change in hardness value is higher than sample 1 and 2 because the force applied is increase to 200 mm/min. The reason why hardness/elastic modulus decrease after tensile test (200 mm/min) is same as previous explanation which is because of rubber surface morphology has shown that the damages on the surface layer due to the tensile test but for tensile test at rate 200 mm/min, we already can see the differences on the microscopic which is much damage on the surface compare to 100 mm/min rate where the boundaries start to break which lead to the decreasing of hardness and elastic modulus value.





`

c) Young modulus

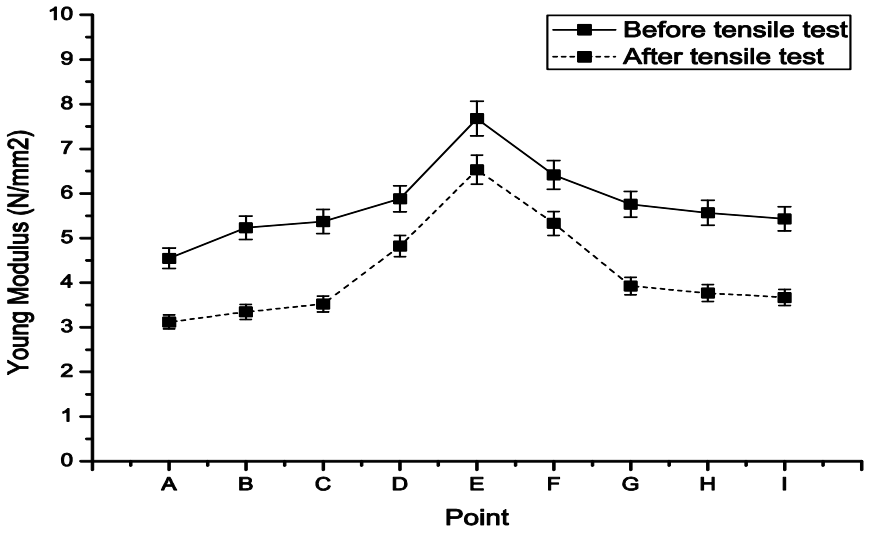


(a)

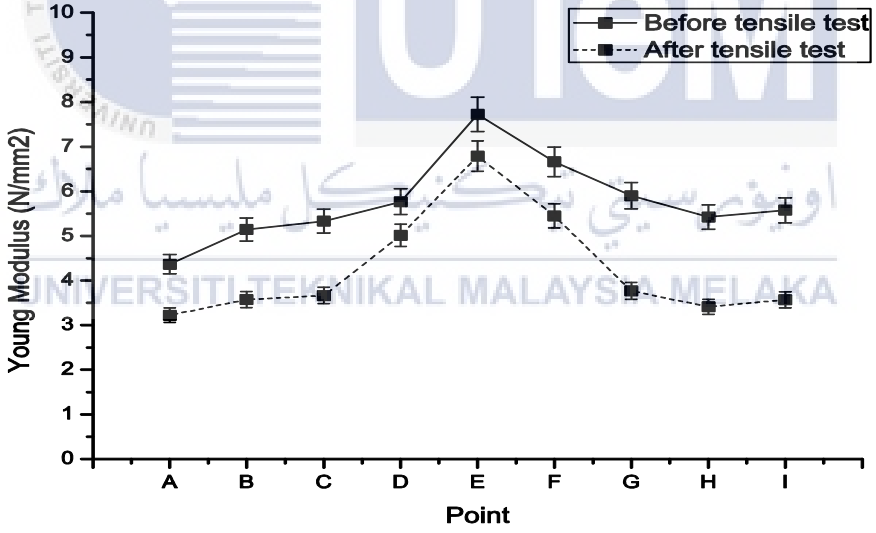


(b)

Figure 4.9: Graph young modulus (a) sample 5 (b) sample 6





`

The recorded elastic modulus (before and after tensile test) at different force for sample 5 and sample 6 was plotted separately in figure 4.9. Tensile test at 200 mm/min have been done to the NR to see the differences between before and after tensile test. As we can see based on the both graph, the young modulus value for before and after tensile test was slightly change as the force increase. The value of elastic modulus for before tensile test is decrease after tensile test. As shown in the figure above, the elastic modulus (before tensile test) for sample 5 was found to be slightly increase from 4.545 to 5.433 and elastic modulus (after tensile test) for sample 5 was also increase from 3.121 3.668. Besides, the elastic modulus (before tensile test) range for sample 6 was found increase from 4.365 to 5.575 and elastic modulus (after tensile test) for sample 6 was also increase from 3.224 to 3.568. For overall, we can see that the young modulus decrease after tensile test 200 mm/min where its created a larger gap in reducing of hardness value compare to 100 mm/min. Related with the statement saying that as stresses increase, Young's modulus may no longer remain constant but decrease, or the material may either flow, undergoing permanent deformation, or finally break (Young & Young, 2019). Small gap between the two graph have been noticed. In addition, much gap between before and after tensile test at point A, B, C, G, H and I. This have been happened to tensile test 100 mm/min but greater gap between before and after tensile have been noticed. This happen because of point position. Point A, B, C located at top of the SMR CV 60 where it located near the tensile test clamp. Surely it will experience much force compare to point D, E and F which located at the middle of sample.





`

### 4.1.4 Tensile test (300 mm/min)

Table 4.4: Hardness and young modulus for tensile test (300 mm/min)

| Point ($mN$) | Sample 7 | | | | Sample 8 | | | |
|---|---|---|---|---|---|---|---|---|
| | Hardness ($HV$) | | Young Modulus ($N/mm2$) | | Hardness ($HV$) | | Young Modulus ($N/mm2$) | |
| | Before Tensile Test | After Tensile Test | Before Tensile Test | After Tensile Test | Before Tensile Test | After Tensile Test | Before Tensile Test | After Tensile Test |
| A(0.1) | 0.028 | 0.019 | 4.665 | 2.583 | 0.029 | 0.018 | 4.586 | 2.612 |
| B(0.2) | 0.029 | 0.020 | 5.172 | 2.722 | 0.031 | 0.022 | 5.132 | 2.811 |
| C(0.4) | 0.034 | 0.023 | 5.243 | 3.044 | 0.033 | 0.025 | 5.321 | 3.023 |
| D(0.6) | 0.039 | 0.035 | 5.876 | 4.186 | 0.037 | 0.032 | 5.755 | 4.105 |
| E(0.8) | 0.047 | 0.044 | 7.912 | 6.553 | 0.050 | 0.046 | 7.932 | 6.646 |
| F(1.0) | 0.034 | 0.030 | 7.112 | 6.057 | 0.040 | 0.035 | 7.366 | 6.121 |
| G(1.2) | 0.032 | 0.022 | 6.211 | 4.554 | 0.037 | 0.029 | 6.121 | 4.223 |
| H(1.4) | 0.030 | 0.020 | 5.957 | 3.831 | 0.035 | 0.025 | 5.976 | 3.799 |
| I(1.6) | 0.027 | 0.020 | 5.575 | 3.091 | 0.030 | 0.021 | 5.118 | 2.997 |





`

a) Load displacement curve

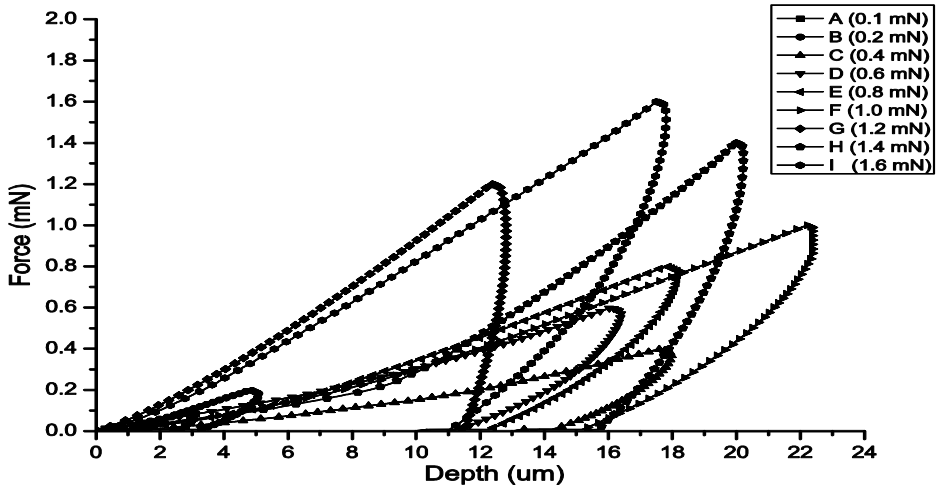


(a)

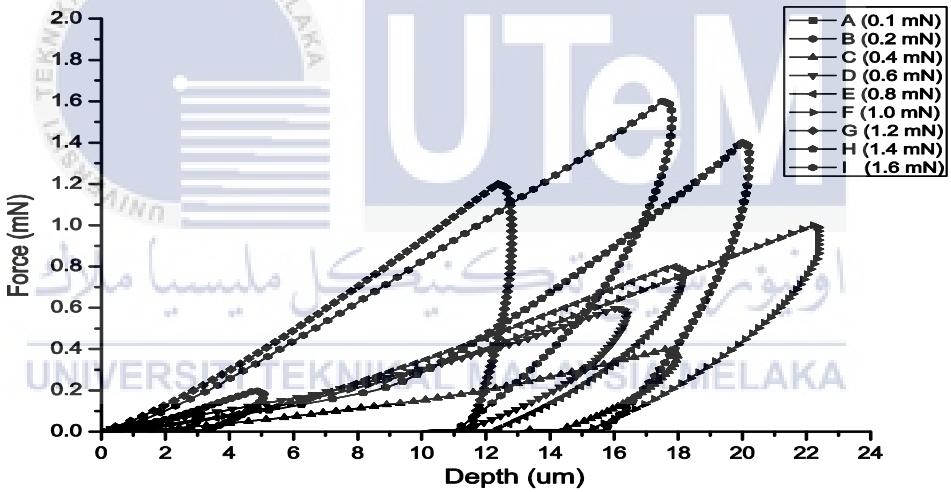


(b)

Figure 4.10: Graph load displacement curve (a) sample 7 (b) sample 8

As shown in figure 4.10, the curves have showed that the compounds have exhibited for different deformation modes depending on the force applied. Together with that, based on the figures above, it was showed the remnant depth at the end of the unloading curve were randomly varies from 2.23 to 15.88 for both sample.



`

b)Hardness

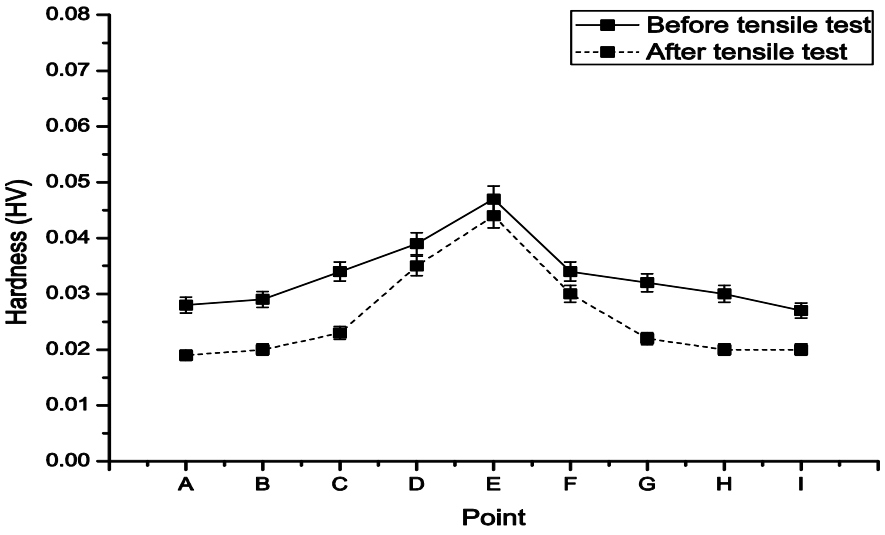


(a)

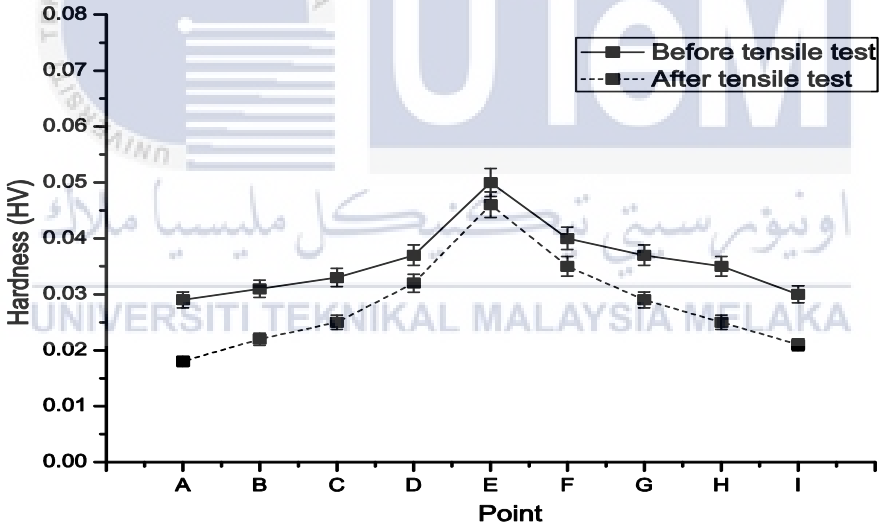


(b)

Figure 4.11: Graph hardness (a) sample 7 (b) sample 8





`

Hardness (before and after tensile test) at different force for sample 7 and sample 8 was plotted separately in figure 4.11. For Sample 7 and 8, tensile test (300 mm/min) have been done to the SMR CV-60 and the data collected before and after test have been plotted and compared. The relationship between the material hardness with the force applied for SMR CV-60 has been presented in figure above. The graph showed that hardness value of SMR CV-60 for before and after tensile test is unpredictable with force from 0.1 $mN$ mN to 1.6 $mN$. The graph have shown a greater gap for hardness value after tensile compare to previous test which is 100 mm/min and 200 mm/min. Based on both graph, we can still see a same trend between sample 7 and sample 8. For overall, we can see that the hardness decrease after tensile test 300 mm/min. Hardness reduce a lot after tensile test 300 mm/min. The change in hardness value is the highest compare to tensile test 100 and 200 mm/min. The reason why hardness/elastic modulus decrease after tensile test (300 mm/min) is same as previous explanation which is because of rubber surface morphology has shown that the damages increase on the surface layer due to the tensile test but for tensile test at rate 300 mm/min, we already can see the differences on the microscopic which is much damage on the surface compare to 100 and 200 mm/min rate where the boundaries start to break which lead to the decreasing of hardness and elastic modulus value.





`

c) Young modulus

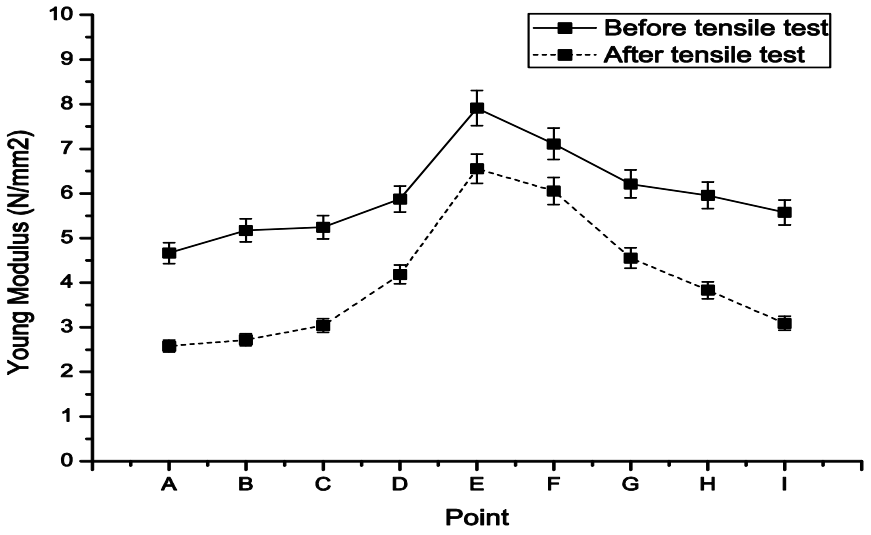


(a)

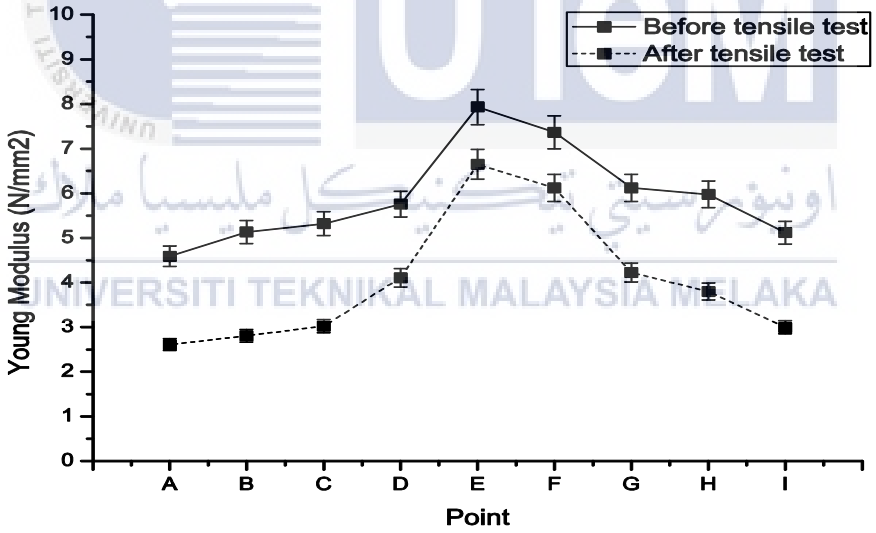


(b)

Figure 4.12: Graph young modulus (a) sample 7 (b) sample 8





`

Tensile test at 300 mm/min have been done to the NR to see the differences between before and after tensile test. As we can see based on both graph, the young modulus value for before and after tensile test was slightly change as the force increase. Based on the figure 4.12, the value of elastic modulus for before tensile test is decrease after tensile test. The elastic modulus (before tensile test) for sample 5 was found to be slightly increase from 4.665 to 5.575 and elastic modulus (after tensile test) for sample 5 was also increase from 2.583 to 3.091. Besides, the elastic modulus (before tensile test) range for sample 6 was found increase from 4.586 to 5.118 and elastic modulus (after tensile test) for sample 6 was also increase from 2.612 to 2.997. For overall, we can see that the young modulus decrease after tensile test 300 mm/min where noticed that graph created a largest gap in reducing of hardness value compare to 100 and 200 mm/min. Furthermore, same as previous tensile test, much gap between before and after tensile test at point A, B, C, G, H and I. Point D, E, F located at the middle of the sample where its experienced less force from the tensile test. While point A, B, C located at top of the SMR CV 60 where it located near the tensile test clamp. Surely it will experience much force compare to point D, E and F which located at the middle of sample





`

### 4.1.5 Heat treatment (100 and 150)

Table 4.5: Hardness and young modulus for heat treatment

| Point ($mN$) | Sample 9 | | | | Sample 10 | | | |
|---|---|---|---|---|---|---|---|---|
| | Hardness ($HV$) | | Young Modulus ($N/mm2$) | | Hardness ($HV$) | | Young Modulus ($N/mm2$) | |
| | Before Heat | After Heat | Before Heat | After Heat | Before Heat | After Heat | Before Heat | After Heat |
| A (0.1) | 0.021 | 0.018 | 4.543 | 4.443 | 0.02 | 0.01 | 4.7 | 4.675 |
| B(0.2) | 0.024 | 0.019 | 5.142 | 5.022 | 0.0212 | 0.012 | 4.432 | 4.451 |
| C(0.4) | 0.025 | 0.022 | 5.267 | 5.657 | 0.031 | 0.015 | 5 | 5.208 |
| D(0.6) | 0.03 | 0.025 | 6.078 | 6.166 | 0.0345 | 0.019 | 5.12 | 4.933 |
| E(0.8) | 0.045 | 0.04 | 8.032 | 7.886 | 0.0465 | 0.017 | 6.9 | 3.132 |
| F(1.0) | 0.041 | 0.035 | 7.346 | 7.223 | 0.035 | 0.023 | 4.833 | 4.634 |
| G(1.2) | 0.038 | 0.033 | 6.166 | 6.011 | 0.0342 | 0.022 | 4.343 | 4.11 |
| H(1.4) | 0.034 | 0.03 | 5.877 | 5.766 | 0.0321 | 0.021 | 4.234 | 4.56 |
| I(1.6) | 0.032 | 0.027 | 5.656 | 5.776 | 0.032 | 0.019 | 4.255 | 4.412 |





`

a) Load displacement curve

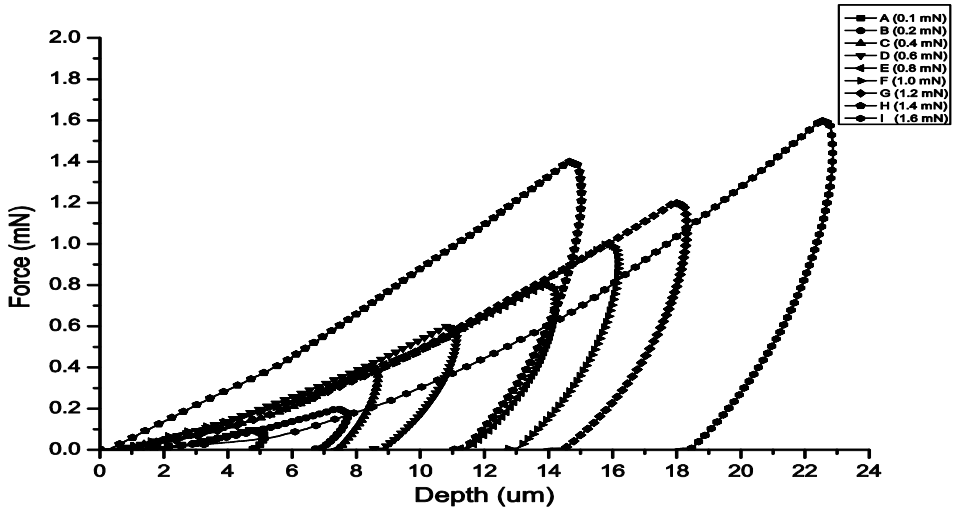


(a)

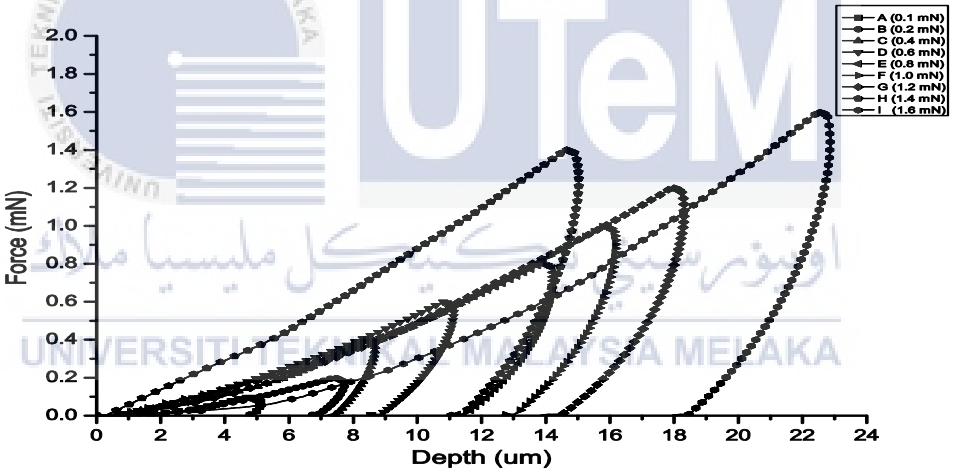


(b)

Figure 4.13: Graph load displacement curve (a) sample 9 (b) sample 10

As shown in figure 4.13, the curves have showed that the compounds have exhibited for different deformation modes depending on the force applied. So, based on the figures above, it was showed the remnant depth at the end of the unloading curve were randomly varies from 2.23 to 18.2 for both sample.





`

b) Hardness

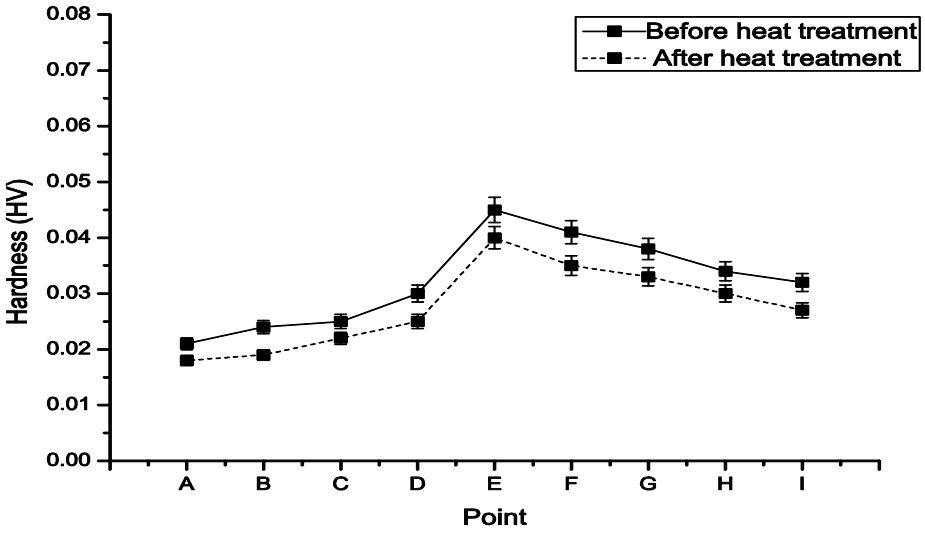


(a)

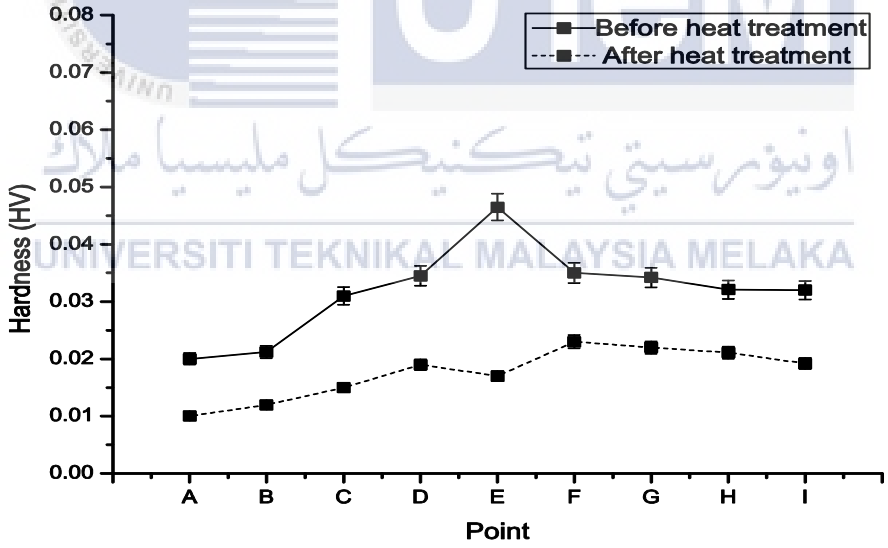


(b)

Figure 4.14**:** Graph hardness (a) sample 9 (b) sample 10





`

The recorded hardness (before and after heat treatment) at different force for sample 9 and sample 10 was plotted separately in figure4.14. 100 ℃ was applied to the sample 9 and 150 ℃ was applied to sample 10. As we can see based on both graph, the hardness value for before and after heat treatment was slightly change as the force increase from 0.1 $mN$ to 1.6$mN$. Most elastomers will undergo significant changes over time when exposed to heat, light, or oxygen (ozone). The hardness (after heat treatment) was lower than hardness (before heat treatment). As we can see, hardness decrease as the heat treatment have been done to both sample. Hardness of rubber also depends on temperature. By raising temperature the free volume of rubber increases and the effective potential barriers for molecular conformations decrease, making the network less stiff and thus causing drop of its hardness (Herrmann, 2004). The hardness (before heat treatment 100 ℃) for sample 9 was increase from 0.021 to 0.032 with the increasing of force and the hardness value (after heat treatment 100 ℃) for sample 9 was a little bit increase from 0.018 to 0.027. In addition, the hardness value (before heat treatment 150 ℃) range for sample 10 was found to be increase from 0.02 to 0.032 and hardness value (after heat treatment 150 ℃) for sample 10 was also increase from 0.01 to 0.0192. So, we can conclude that heat treatment 150 ℃ shows bigger gap for before and after heat treatment compare to heat treatment 100 ℃ but there is a significant decrease in the value of hardness at point E compare to other point. As a result of observation in sample 10, this occurs because of the sample 10 surface starts to melt because there is a liquid on the surface of the sample 10. This happens because heat treatment is 150 which is close to the value of melting point for natural rubber which is rubber begins to melt at approximately 180 degrees Celsius (Herrmann, 2004).





`

c) Young modulus

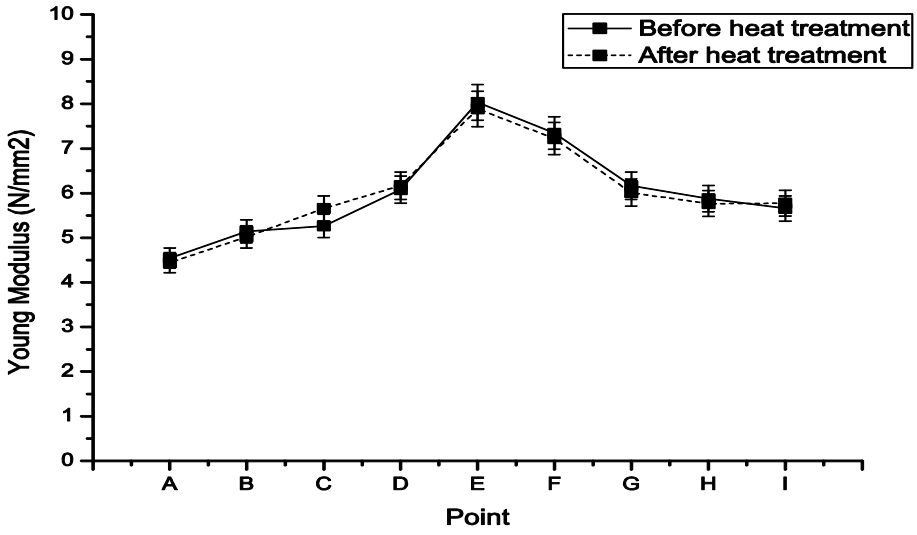


(a)

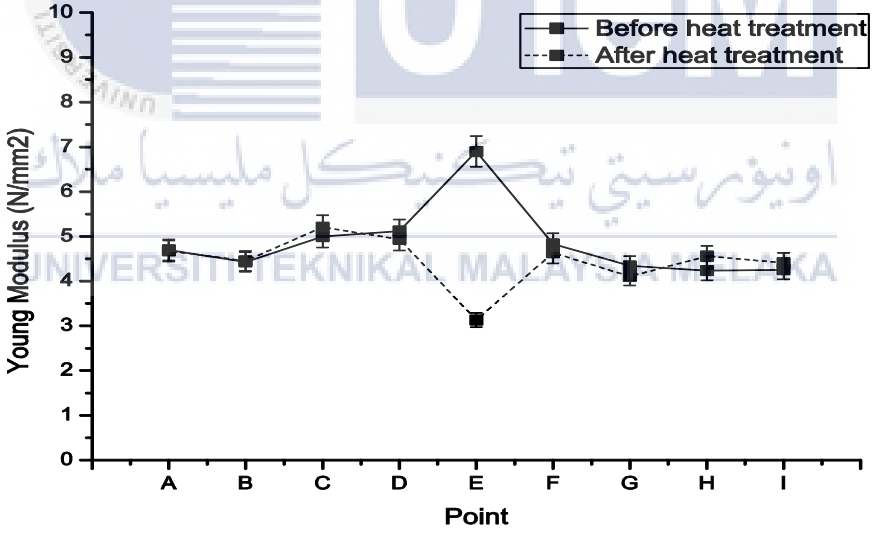


(b)

Figure 4.15: Graph young modulus (a) sample 9, (b) sample 10





`

The recorded young modulus (before and after heat treatment) at different force for sample 9 and sample 10 was plotted separately in figure 4.15. 100 ℃ was applied to the sample 9 and 150 ℃ was applied to sample 10. Based on the both graph, the young modulus value for before and after heat treatment was slightly change as the force increase from 0.1 to 1.6 $mN$. Most elastomers will undergo significant changes over time when exposed to heat, light, or oxygen (ozone). The study of effect of temperature on Young's modulus is extremely important for the strength under high temperature. Therefore, the relationship between Young's modulus and temperature is relatively complicated. When the temperature increases, the atomic thermal vibrations increase, and this will cause the changes of lattice potential energy and curvature of the potential energy curve, so the Young's modulus will also change (Li, Wang, Li, & Fang, 2011). The young modulus (after heat treatment) was lower than hardness (before heat treatment). As we can see, young modulus decrease as the heat treatment have been done to both sample and with the increase of temperature, the material will have a volume expansion. Thus we know that the change of Young's modulus with temperature involves two aspects; one is the atomic binding force, and the other is the volume of material. There is no much comparison between young modulus value for before and after heat treatment maybe because of elastomers can be deformed to very large strains and the spring back elastically to the original length, a behaviour first observed in natural rubber. So, heat treatment at 100 ℃ still not enough to change the young modulus value but young modulus drop in large amount at point E for sample 10. As a result of observation in sample 10, this occurs because of the sample 10 surface starts to melt because there is a liquid on the surface of the sample 10. This happens because heat treatment is 150 ℃ which is close to the value





`

of melting point for natural rubber which is Rubber begins to melt at approximately 180 degrees Celsius (Herrmann, 2004).

## 4.2 Chapter summary

In this study, SMR – CV 60 has been used as a sample of experiment. Through the nanoindentation test, (hardness and young modulus) for 3 different types of NR conditions which is normal test, tensile test and heat treatment with different force were recorded and analysed. All finding in this study was presented and discussed in details in this chapter





`

# CHAPTER 5

# CONCLUSION

## 5.0 Introduction

This chapter will be discussing on the conclusion and recommendation for the future work to further improvement of this experiment.

## 5.1 Conclusion

The present study was designed to determine the mechanical properties (hardness and young modulus) of NR with different force applied (0.1, 0.2, 0.4, 0.6, 0.8, 1.0, 1.2, 1.4 and 1.6) $mN$ through nanoindentation testing. In this study, there is only 1 types of NR used which is the Standard Malaysian Rubber with Constant Viscosity – 60 (SMR CV-60). The mechanical studies of the rubber was determined using nanoindentation testing with three different test condition which is normal, tensile and heat treatment. The normal test refer to original condition of rubber without any testing before using nanoindentation test. Tensile test was conducted at room temperature by stretching the specimen at rate of 100, 200 and 300 mm/min before conduction nanoindentation testing. Heat treatment was carried out at temperature of 100 and 200 before conducting nanoindentation testing. The reason to conduct 3 test above was to determine the hardness and young modulus for before and after test.

Based on the result obtained, it can be concluded that the properties of the NR were highly affected by the force applied. The findings of this study are as follow:





`

- For normal test, the depth penetration increase as the force increase. The hardness/young modulus is unpredictable as the force increase but graph showing an increasing trend for hardness value. The highest hardness/young modulus was at point E which is located at the middle of the sample.
- For tensile test 100 mm/min, the depth penetration also increase as the force applied increase. The hardness/young modulus decreases after tensile test 100 mm/min. Point A, B, C, G, H and I recorded higher drop in hardness/young modulus value compare to point D, E and F due to point position.
- For tensile test 200 mm/min, the depth penetration also increase as the force applied increase. The hardness/young modulus decreases after tensile test 200 mm/min but hardness drop after 200 mm/min was higher compare to tensile test 100 mm/min. The hardness/young modulus decreases after tensile test 100 mm/min. Point A, B, C, G, H and I recorded higher drop in hardness/young modulus value compare to point D,E and F due to point position but higher drop compare to 100 mm/min.
- For tensile test 300 mm/min, the depth penetration also increase as the force applied increase. The hardness/young modulus decreases after tensile test 300 mm/min but hardness drop after 300 mm/min was higher compare to tensile test 100 and 200 mm/min. Point A, B, C, G, H and I recorded higher drop in hardness/young modulus value compare to point D, E and F due to point position but higher drop compare to 100 and 200 mm/min.
- Lastly, for heat treatment, the depth penetration also increase as the force applied increase. For sample 9 where heat treatment at 100, the hardness decrease after





`

heat treatment for both sample 9 and 10 but for sample 10, at point E, which is located at the middle of the sample, hardness decrease a lot because the surface at the middle start to melt after heat treatment. The young modulus value were almost the same as normal test for sample 9 where not much change for young modulus value.

## 5.2 Future Work

In the future invention of this experiment that can be suggested is to increase the force applied by the nano indenter in order to see much differences between each point. Second, to add other NR sample for example ENR, so comparison in mechanical testing can be seen clearly. The technique to determined mechanical properties (hardness and young modulus) need to be added such as micro-hardness tester and shore hardness. By adding the technique, data will be more accurate in the future.



## 5.3 Summary

The conclusion and the future work are needed to finalize the overall experiment. It is also important to summarize the result obtain. This chapter is important because, it help to overcome the problem and improve the efficiency of this experiment.



`

# REFERENCES


Baker, C. S. L., Gelling, I. R., & Samsuri, A. B. I. N. (n.d.). Epoxidised Natural Rubber, *1*(2), 135–144.

Broitman, E. (2017). Indentation Hardness Measurements at Macro-, Micro-, and Nanoscale: A Critical Overview. *Tribology Letters*, *65*(1), 1–18. https://doi.org/10.1007/s11249-016-0805-5

Carter, G. F., & Giles F. Carter and Donald E. Paul, editors. (1991). *Materials Science and Engineering*. A S M International. Retrieved from https://books.google.com.my/books?id=3xzzJQjSqjsC

Herrmann, K. (2004). Long-Term Stability of Rubber Hardness Reference Blocks. Retrieved from https://www.reference.com/science/melting-point-rubber-7866027e204cc4a4

Ibrahim, R. A. Ã. (2008). ARTICLE IN PRESS Recent advances in nonlinear passive vibration isolators, *314*, 371–452. https://doi.org/10.1016/j.jsv.2008.01.014

Li, W., Wang, R., Li, D., & Fang, D. (2011). A Model of Temperature-Dependent Young ' s Modulus for Ultrahigh Temperature Ceramics, *2011*. https://doi.org/10.1155/2011/791545

Lu, L., Wang, L. B., Ding, B. Z., & Lu, K. (2000). Materials research. *Materials Research*, *6*(2), 1–4.

Moharrami, N. (2013). Extracting Reliable Mechanical Properties using the Nanoindentation Technique, (December).

Page, T. F., & Hainsworth, S. V. (1993). Using nanoindentation techniques for the characterization of coated systems: a critique. *Surface and Coatings Technology*, *61*(1–3), 201–208. https://doi.org/10.1016/0257-8972(93)90226-E




`

Poon, B., Rittel, D., & Ravichandran, G. (2008). An analysis of nanoindentation in elasto-plastic solids. *International Journal of Solids and Structures*, *45*(25–26), 6399–6415. https://doi.org/10.1016/j.ijsolstr.2008.08.016

*Rubber as a Construction Material for Corrosion Protection*. (n.d.). Retrieved from https://onlinelibrary.wiley.com/doi/book/10.1002/9780470893197

Salim, M. A., Putra, A., & Abdullah, M. A. (2015). Horizontal displacement of laminated rubber-metal spring for engine isolator. *ARPN Journal of Engineering and Applied Sciences*, *10*(17), 7841–7846.

Salim, M. A., Putra, A., Mansor, M. R., Musthafah, M. T., Akop, M. Z., & Abdullah, M. A. (2016). Analysis of Parameters Assessment on Laminated Rubber-Metal Spring for Structural Vibration. *IOP Conference Series: Materials Science and Engineering*, *114*(1). https://doi.org/10.1088/1757-899X/114/1/012014

Salim, M. A., Putra, A., Mansor, M. R., Musthafah, M. T., Akop, M. Z., Abdullah, M. A., … Shaharuzaman, M. A. (2016). Sustainable of Laminated Rubber-Metal Spring in Transverse Vibration. *Procedia Chemistry*, *19*, 203–210. https://doi.org/10.1016/j.proche.2016.03.094

Schaefer, R. J. (n.d.). Mechanical Properties Of Natural Rubber

The, O., & One, I. (n.d.). EXPERIMENT 3 : HARDNESS TEST, 3–10.

Wong, E. T., & Louis, D. N. (2001). *Case Records of the Massachusetts General Hospital Case 8-2001. New England Journal of Medicine* (Vol. 344). https://doi.org/10.1111/j.1835-9310.1997.tb00178.x

Wu, H., Li, Y., Tang, X., Hussain, G., Zhao, H., Li, Q., & Adedotun, A. (2015). Nano-mechanical characterization of plasma surface tungstenized layer by depth-sensing nano-indentation measurement. *Applied Surface Science*, *324*, 160–167. https://doi.org/10.1016/j.apsusc.2014.10.085

BEN Ghorbal, G., Tricoteaux, A., Thuault, A., Louis, G., & Chicot, D. (2017). Mechanical characterization of brittle materials using instrumented indentation with Knoop indenter. *Mechanics of Materials*, *108*, 58–67. https://doi.org/10.1016/j.mechmat.2017.03.009



`

Broitman, E. (2017). Indentation Hardness Measurements at Macro-, Micro-, and Nanoscale: A Critical Overview. *Tribology Letters*, *65*(1), 1–18. https://doi.org/10.1007/s11249-016-0805-5

Bull, S. J. (2002). Extracting hardness and Young's modulus from load-displacement curve. *Zeitschrift Fur Metallkunde*, *93*(9), 870–874. https://doi.org/10.3139/146.020870

Bullock, B. P., & Burkhart, H. E. (2005). An evaluation of spatial dependency in juvenile loblolly pine stands using stem diameter. *Forest Science*, *51*(2), 102–108. https://doi.org/10.1007/978-1-4419-9872-9

Chen, J., & Bull, S. J. (2006). A critical examination of the relationship between plastic deformation zone size and Young's modulus to hardness ratio in indentation testing. *Journal of Materials Research*, *21*(10), 2617–2627. https://doi.org/10.1557/jmr.2006.0323

Chinn, R. E., & Energy, N. (2009). HARDNESS , (October), 29–31.

Field, J. S., & Swain, M. V. (1995). Determining the mechanical properties of small volumes of material from submicrometer spherical indentations. *Journal of Materials Research*, *10*(1), 101–112. https://doi.org/10.1557/JMR.1995.0101

Fischer-Cripps, A. C. (2004). Multiple-frequency dynamic nanoindentation testing. *Journal of Materials Research*, *19*(10), 2981–2988. https://doi.org/10.1557/JMR.2004.0368

Knoop, F., Peters, C. G., & Emerson, W. B. (1939). A sensitive pyramidal-diamond tool for indentation measurements. *Journal of Research of the National Bureau of Standards*, *23*(1), 39. https://doi.org/10.6028/jres.023.022

Lawn, B. R., & Fuller, E. R. (1975). Equilibrium penny-like cracks in indentation fracture. *Journal of Materials Science*, *10*(12), 2016–2024. https://doi.org/10.1007/BF00557479

Lu, L., Wang, L. B., Ding, B. Z., & Lu, K. (2000). Materials research. *Materials Research*, *6*(2), 1–4.

Lucca, D. A., Herrmann, K., & Klopfstein, M. J. (2010). Nanoindentation: Measuring methods and applications. *CIRP Annals - Manufacturing Technology*, *59*(2), 803–819. https://doi.org/10.1016/j.cirp.2010.05.009



`

Moharrami, N. (2013). Extracting Reliable Mechanical Properties using the Nanoindentation Technique, (December).

Page, T. F., & Hainsworth, S. V. (1993). Using nanoindentation techniques for the characterization of coated systems: a critique. *Surface and Coatings Technology*, *61*(1–3), 201–208. https://doi.org/10.1016/0257-8972(93)90226-E

Pharr, G. M. (1998). Measurement of mechanical properties by ultra-low load indentation. *Materials Science and Engineering: A*, *253*(1–2), 151–159. https://doi.org/10.1016/S0921-5093(98)00724-2

Poon, B., Rittel, D., & Ravichandran, G. (2008). An analysis of nanoindentation in elasto-plastic solids. *International Journal of Solids and Structures*, *45*(25–26), 6399–6415. https://doi.org/10.1016/j.ijsolstr.2008.08.016

Salim, M. A., Putra, A., & Abdullah, M. A. (2015). Horizontal displacement of laminated rubber-metal spring for engine isolator. *ARPN Journal of Engineering and Applied Sciences*, *10*(17), 7841–7846.

Salim, M. A., Putra, A., Mansor, M. R., Musthafah, M. T., Akop, M. Z., & Abdullah, M. A. (2016). Analysis of Parameters Assessment on Laminated Rubber-Metal Spring for Structural Vibration. *IOP Conference Series: Materials Science and Engineering*, *114*(1). https://doi.org/10.1088/1757-899X/114/1/012014

Salim, M. A., Putra, A., Mansor, M. R., Musthafah, M. T., Akop, M. Z., Abdullah, M. A., … Shaharuzaman, M. A. (2016). Sustainable of Laminated Rubber-Metal Spring in Transverse Vibration. *Procedia Chemistry*, *19*, 203–210. https://doi.org/10.1016/j.proche.2016.03.094

Schuh, C. A. (2006). Nanoindentation studies of materials. *Materials Today*, *9*(5), 32–40. https://doi.org/10.1016/S1369-7021(06)71495-X

Wong, E. T., & Louis, D. N. (2001). *Case Records of the Massachusetts General Hospital Case 8-2001*. *New England Journal of Medicine* (Vol. 344). https://doi.org/10.1111/j.1835-9310.1997.tb00178.x

Wu, H., Li, Y., Tang, X., Hussain, G., Zhao, H., Li, Q., & Adedotun, A. (2015). Nano-mechanical characterization of plasma surface tungstenized layer by depth-sensing nano-indentation measurement. *Applied Surface Science*, *324*, 160–167. https://doi.org/10.1016/j.apsusc.2014.10.085



`